Physical Concepts of Copolymerization of Microtubules in the Presence of Anti-mitotic Agents

Mitra Shojania Feizabadi

Dissertation submitted to the Faculty of the
Virginia Polytechnic Institute and State University
in partial fulfillment of the requirements for the degree of

Doctor of Philosophy
in
Physics

Prof. William B. Spillman Jr., Chair
Prof. Tetsuro Mizutani
Prof. Jimmy Ritter
Prof. Richard Walker
Prof. Guy Indebetouw

April 29, 2005
Blacksburg, Virginia

Keywords: microtubule, dynamic instability, antimitotic drugs

Dynamics of Microtubules in the Presence of Anti-mitotic drugs

Mitra Shojania Feizabadi

(ABSTRACT)

Microtubules play a key role in the process of cell division. They can be polymerized by tubulin subunits which are proteins. These microtubules show a non equilibrium behavior in their dynamics. They are a good target of anti-mitotic agents. These agents effect the dynamic parameters and polymerization of microtubules and therefore control the process of cell division.

It is necessary to develop a frame-work in which theoretical and experiment research works cohesively in order to generate accurate descriptions of the different biological components and the way they interact with each other. This study will further the theoretical research by expressing the copolymerization of microtubules mathematically.

T-tubulins are the building blocks of microtubules. The polymerization of microtubules in the presence of pure T-tubulin is expressed mathematically by the Hill's model. In the presence of anti-mitotic drugs, two spices of subunits will exist in the solution which have the ability to be polymerized. The polymerization process that occurs in such an environment is called coploymerization. The intention of this work is to:

- Extend the existing mathematical model of polymerization in the presence of two species of subunits.
- Investigate the possibility of the existence of analytical solutions for kinetic equations under the specific conditions.
- Use the extended model using simulations to calculate the biological quantities involved in the process of copolymerization and compering the results with experimental measurements.

Based on the model presented by Hill, a new set of equations for the dynamics of microtubules in the presence of anti-mitotic drugs is built in this thesis. In low concentrations of one of the anti-mitotic drugs, colchicine, dynamical equations are analytically solvable in the steady state. With the help of the stationary solutions, one of the measurable biological parameters is calculated numerically. The simulation results were consistent with data reported in previous biological experiments, adding strength to the potential validity of the assumptions in this model. The next phase of this project extended theoretical models to the interaction of other drugs like taxol or high concentrations of colchicine with the microtubule lattice. Solving the dynamical equations in the latter case was dependent on the bio-statistical parameters. Under specific conditions, the equations can be solved analytically. Results obtained in this phase were also compatible with experimental results.

Contents

List of Figures

Dedication

To my parents

Acknowledgments

I would like to express my sincere appreciation to Prof. William B. Spillman Jr. for giving me a chance to work with him. Prof. Spillman is a good researcher as well as a good teacher and without his constant help and advice this work has not been completed.

I also want to thank the members of my graduate advisory committee: Dr. Richard Walker, Dr. Jimmy Ritter, Dr. Tetsuro Mizutani, Dr. Guy Indebetouw for all of their advise and efforts to complete this work.

I would like to thank the physics department for their financial support and giving me the opportunity to improve my teaching skills by being a graduate teaching assistant.

Also, a special thank you goes to Mrs.Chris Thomas who was a great help and support during my study in Virginia tech.

Most importantly, I would like to thank my parents and my brothers for all they love and supports.

Chapter 1

Structure and Dynamics of Microtubules

1.1 Introduction

Microtubules (MTs) are cylindrical filaments used in cells for many different purposes such as intercellular transport, and are made up of a complex of guanosine triphosphate (GTP) and tubulin (T-tubulin). Microtubules in cells generally display non-equilibrium dynamics. They assemble, disassemble or re-arrange in a time scale of minutes. The rich non-equilibrium dynamics of microtubules, including nucleation and polymerization kinetics, are attracting considerable attention, both experimentally and theoretically [1]-[15]. Various experimental and theoretical studies have been aimed at extracting characteristic features of the life history of microtubules in order to build mathematical models that can be used to gain insight into the physical processes involved [16]. The growth of microtubules through so-called dynamic instability was analyzed in a simple theoretical model in a series of papers by Hill and Chen [17]-[18], and much more recently by Dogterom et al. [11]. The effects of temperature and tubulin concentration on dynamic variables were investigated by Fygenson et al. [19]. They found that dynamic parameters and assembly processes of microtubules are relevant under biological conditions. Dogterom et al. presented a theoretical analysis to show how the dynamic instability of microtubules in combination with microtubule polymerization forces produces a microtubule organizing center [20]. Flyvbjerg et al. modeled the competition between added GTP and

tubulin at the growing tip, as well as the hydrolysis of GTP in microtubule bodies [21]. Another interesting phenomenon is the dampened periodic oscillation of microtubules studied by Sept [22]. These oscillations are due to the variation in the total amount of assembled tubulin and do not reflect a change in length of individual microtubules. Some of Sept's first results showed how microtubules would switch from normal monatomic growth to oscillations when either the tubulin or GTP concentration was increased [15]. Sept et al. presented a model for microtubule oscillation based on a set of chemical reaction equations [22].

Two fundamental mathematical models in the dynamics of microtubules are Hill's two-state model [17] and Freed's model [23], which is Hill's generalized model. These two models are analytically solvable in the steady state and generally capable of describing the dynamics of the system. These two models are the building blocks of recent dissertations and will be reviewed in the next chapter.

The following section briefly introduces the structure of microtubules and the role of microtubules in cellular functions. It also explains the formation of microtubules and discusses dynamic instability, which is the dominant mechanism governing microtubule polymerization. Also, the bound state, the steady state, and the unbound state will be defined. The next section addresses why microtubules are important and presents the main objectives of this work. The philosophy and importance of mathematical modeling for a biological system will be discussed next. The overview of this dissertation is given in the last section.

1.2 Microtubule structure and dynamic instability

One of the most important issues of molecular biophysics is the complex and multi-functional behavior of the cytoskeleton. The interior of living cells is structurally organized by cytoskeleton networks of filamentous protein polymer: microtubules, actin, and intermediate filaments, with motor proteins providing the force and directionality needed for transport. The thickest and perhaps most multi-functional of all cytoskeletal filaments are microtubules, which are involved in different cellular activities and are found in nearly all eukaryotic cells. Microtubules can be assembled from pure GTP-tubulin in

vitro [24]. Microtubules are involved in a number of specific cellular functions, such as:

- Organelle and particle transport inside cells through the use of motor proteins;
- Locomotion or cell mobility, when arranged in geometric patterns inside flagella and cilia; and
- Formation during cell division of the mitotic spindles required for chromosome segregation.

Fig 1.1 shows different phases of cell division. In early metaphase, most chromosomes have congressed to the equator to form the metaphase plate. In anaphase, the duplicated chromosomes have separated and move toward the spindle poles to form the two daughter cells. In telophase, the separated chromosoms have reached the spindle poles and the cell is dividing to form two daughter cells [26]. The highly dynamic microtubules in the spindle are required for all stages of mitosis: first, for the timely and correct attachment of chromosomes at their kinetochores to the spindle after nucleation (envelope breakdown); second, for the complex movement of chromosomes called congression that brings them to their properly aligned positions at the metaphase plate; and last, for the sychronous separation of the chromosomes in anaphase [26]

The elementary building block of a MT is an α -β dimer whose dimensions are 4 by 5 by 8 nm. The dimers assemble into a cylindrical structure that typically has 13 protofilaments. The outer diameter of a MT is 25 nm and the inner diameter is 15 nm [26]. The monomer mass is about 55 KDA. A schematic view of microtubule formation is shown in Fig 1.2. This structure is the most common structure of a microtubule, although doublet microtubules have also been observed in some special cells.

Tubulin assembly into microtubules is a reversible process which involves a continuous exchange between the soluble and the polymer tubulin populations. The onset of microtubule assembly depends on temperature [19], concentration of tubulin in the cytoplasm, and the supply of biochemical energy in the form of GTP. GTP-tubulin will start to polymerize when a threshold concentration exists. The critical concentration is the threshold concentration at which GTP-tubulin will polymerize into microtubules in vitro. The critical concentration is only a potential problem in vitro because

the cell must always maintain a high enough concentration of α-β dimers to form microtubules. α tubulin binds GTP irreversibly and β tubulin binds GTP reversibly. This association to GTP is essential for tubulin dimers to polymerize into microtubules.

Microtubule assembly proceeds in two phases: nucleation and elongation. Nucleation occurs in the presence of tubulin, Mg++, and GTP at $37C$. Microtubule length may range from hundreds of nanometers to micrometers. Dimers polymerize head-to-tail into profilaments and each MT polymer is polarized. The plus end is the fast assembly end and the minus end is the slow assembly end. In living cells, the polarity of microtubules lends organization to the cell. In undifferentiated cells in vivo, microtubule minus ends are believed to be anchored at the centrosome, while their plus ends radiate out to the cell periphery in the interphase array, or toward the chromosomes in the mitotic spindle. Fig 1.3. shows a schematic view of microtubules in cells.

Microtubules are intrinsically dynamic polymers that display non-equilibrium behavior both in vitro and in vivo [1]. One such nonequilibrium behavior that is important in cells is called dynamic instability, in which microtubule ends stochastically switch between growing and shrinking states [1],[27, 28],[29]. After nucleation, a microtubule becomes elongated for a variable period of time before undergoing an abrupt transition (catastrophe) to rapid shrinking. A microtubule in the rapid shortening phase either completely depolymerizes back to a nucleation site in vitro, or undergoes an abrupt transition (rescue) back to the elongation phase. Transition between phases is abrupt, stochastic. A life history diagram for an individual microtubule is presented in Fig 1.4.

Experimental evidence shows that:

- The rate of elongation is proportional to tubulin concentration up to high concentrations of tubulin, where this dynamic parameter is independent of the amount of tubulin in solution [30].
- The plus end association rate constant for elongation is two-fold greater than the minus end value.
- Plus and minus end microtubules exhibit significant dissociation rate during elongation.
- Microtubules occasionally pause during both elongation and rapid shrinking.

- High concentrations of tubulin reduce the frequency of catastrophe and increase the frequency of rescue at both ends.
- The frequency of catastrophe is slightly greater at the plus end.
- The frequency of rescue is greater at the minus end.

The frequency of catastrophe for specific tubulin concentrations can be calculated by summing the elongation times for all microtubules observed and dividing this time into the number of observed catastrophes. A similar method can be used to calculate the frequency of rescue [29]. A simple cycle of MT assembly and disassembly is illustrated in Fig 1.5. Fig 1.6 gives an overview of the chemical reactions involved in this cycle.

The molecular basis of dynamic instability is thought to be some form of cap that stabilizes the plus end of an elongation microtubule. The favored model is the GTP cap as proposed by Mitchison, which is based on earlier ideas that GTP hydrolysis and microtubule assembly might not occur simultaneously. It has been well established that GTP-tubulin adds to the end of an elongating microtubule [29]. The GTP cap model postulates that this hydrolysis produces a labile core of GDP-tubulin within the microtubule, which is capped at the elongation end by a more stable region of GTP-tubulin subunits (Figure 1.7). Catastrophe is the loss of the GTP cap, and rescue is the recapping of a GDP-tubulin end during rapid shrinking.

In practice, microtubule growth is limited only by the size of the container or by free tubulin subunit depletion. In the unbound state, the conditions are such that, on average, microtubules keep elongating with time, although each microtubule can alternately grow and shrink. Another situation, called the bound state, occurs when the ensemble of microtubules does not grow on average; microtubules tend to disassemble all the way back to the nucleation site. Yet, at any time, a finite fraction of surviving microtubules is observed because of the continued re-nucleation at the nucleation site. This gives rise to a steady state, with a well defined distribution of microtubule lengths, which we call the bound state of microtubule assembly Fig. 1.8.

1.3 Why microtubules are important

Microtubules are important in the process of mitosis, during which the duplicated chromosomes of a cell are separated into two identical sets before cleavage of the cell into two daughter cells. Their importance in mitosis and cell

division makes microtubules an important target for anticancer drugs. Drugs which inhibit or destabilize microtubule formation have been used successfully in the treatment of cancer [25]. Microtubules seem to be a favorite target of naturally-occurring, presumably self-protective, toxic molecules that are produced by a large number of plants and animals, ranging from algae to sea hares. Microtubule-targeted anticancer drugs are usually classified into two main groups. One group, known as the microtubule-destabilizing agents, inhibits microtubule polymerization at high concentration and include several components such as the Vinca alkaloids, colchicine and combretastins which are used clinically or are under clinical investigation for treatment of cancer [25]. Paclitaxel, docetaxel, discodermolide are in the second main group of microtubule-target drugs. This group inhibits microtubule polymerization.

In fact, this kind of classification is not accurate enough because drugs that increase or decrease microtubule polymerization at high concentrations suppress microtubule dynamics at very low concentrations. The microtubule-targeted drugs affect microtubule dynamics in several different ways. The difference in the way that various drug classes modulate dynamics seems to specify to what extent and how the proliferation of a tumor cell will be inhibited. Suppression of spindle-microtubule dynamic instability by antimitotic drugs may slow progression from metaphase into anaphase [25]. To improve the understanding and clinical effectiveness of antimitotic drugs, it is helpful to examine them from mathematical point of view. Also, understanding why some drugs often work well in specific type of cancer and whether different combination of drugs can help to modulate the polymerization of microtubules are some of the open questions in this field.

1.4 Mathematical modeling: philosophy and importance

This section describes briefly the philosophy of mathematical model of the dynamics of microtubules in the presence of antimitotic drugs.

Mathematical modeling provides a framework to investigate real conditions in a systematic manner. Observations, experiments, data collection, formalization of properties, mathematization resulting in a mathematical model, model analysis, interpretation, comparison and predictions are the sequential steps in mathematical modeling.

Mathematical modeling is an iterative process. For example, after comparing a model to the data collected, one might go back a few steps to reformulate the model. In fact, justifying the assumptions and hypothesis is always a part of modeling to reach to as accurate a model as possible. Analysis of the mathematical model is an inseparable part of modeling, which can include both theoretical and computational difficulties. Although formidable obstacles can still arise, they are much less critical in modeling today than in the past.

There are two types of mathematical modeling: descriptive and conceptual. Descriptive models are designed to explain observed phenomena mathematically and will be the focus of this study. Conceptual models are constructed to elucidate difficult points in some scientific theory.

In the past, several mathematical models were presented for the dynamics of microtubules made of pure tubulin [17]-[18]. This work will gradually build a new model for the dynamics of microtubules in the presence of antimitotic drugs. The first stage will use the most simple assumptions and then will expand to complicated conditions and a more complex model.

In the comparison stage of this modeling, one of the biological quantities, steady state polymer mass, will be investigated numerically.

1.5 Overview of the dissertation

This dissertation is arranged as follows:

- Chapter 2 first reviews mathematical models for polimerization of microtubules with pure tubulin. Next, a perspective on the mechanism of interaction of microtubules with antimitotic drugs at low concentrations is presented. By making simplifying assumptions, the kinetic equations will be extended and a new mathematical model for copolymerization of microtubules in the presence of substiochiometric levels of antimitotic drugs will be built. The behavior of free T-tubulin concentration in the microtubule steady state and in the presence of colchicine will then be investigated. It will be assumed that there is an excess of GTP (guanosine triphosphate) available in the solution, and that the D-tubulin in the solution will exchange its unit of GDP (guanosine diphosphate) with a unit of GTP. By numerical analysis, the concentration of T-tubulin in the steady state as a function of regeneration

rate is investigated in the presence and absence of colchicine. Results show that low concentrations of colchicine in the steady state do not significantly alter the amount of total free T-tubulin concentration or the polymer mass, in good agreement with experimental observations.

- Chapter 3 develops the mathematics to express the copolymerization of microtubules in the presence of suprastoichiometric levels of antimitotic drugs, including colchicine. Bio-statistical parameters are introduced in this chapter as necessary tools for mathematical calculations.

  The possibility of finding an analytic solution for steady state in this case will be discussed. This chapter will also investigate the behavior of polymer mass in the steady state and under specific conditions.

- Chapter 4 will open a new window to another type of microtubule dynamics which can happen only in the presence of minus ends of microtubules. The treadmilling effect will be introduced in this chapter. The continuous form of the dynamic equations will be expressed as well. The treadmilling steady state in a regenerative system will be investigated from a mathematical point of view.

- Chapter 5 presents closing remarks.

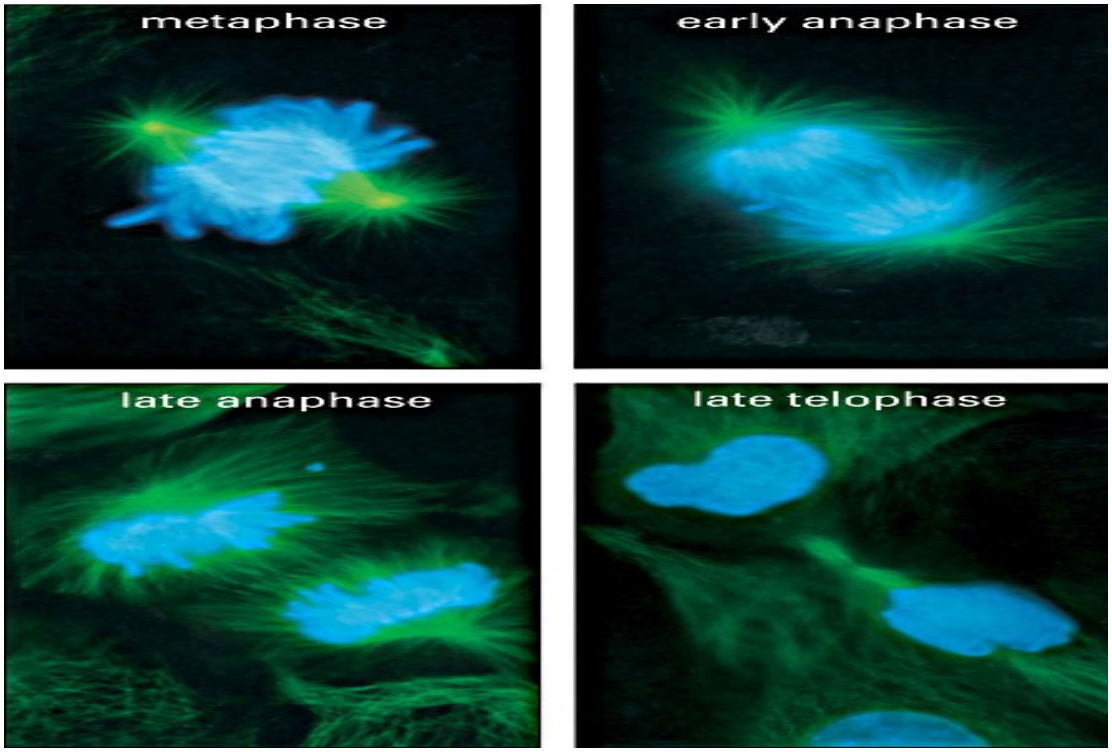

Figure 1.1: Different stages of cell division. In early metaphase, most chromosomes have congressed to the equator to form the metaphase plate. In anaphase, the duplicated chromosomes have separated and moved toward the spindle poles to form the two daughter cells. In telophase, the separated chromosoms have reached the spindle poles and the cell division to form two daughter cells [26].

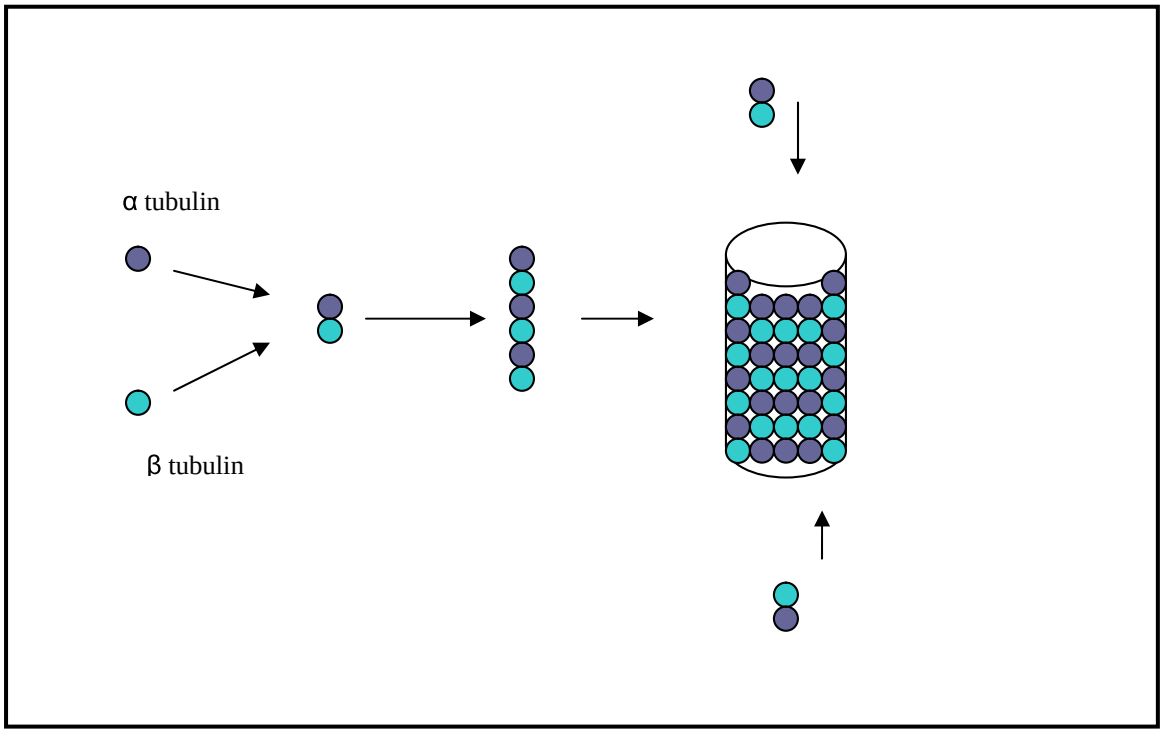

Figure 1.2: Dimers of α and β tubulin assemble to form a short microtubule nucleus. Nucleation is followed by elongation of the microtubule at both ends to form a cylinder that is composed of tubulin dimers arranged head to tail in 13 protofilaments. Each microtubule has a plus (+) end and a minus (−) end.

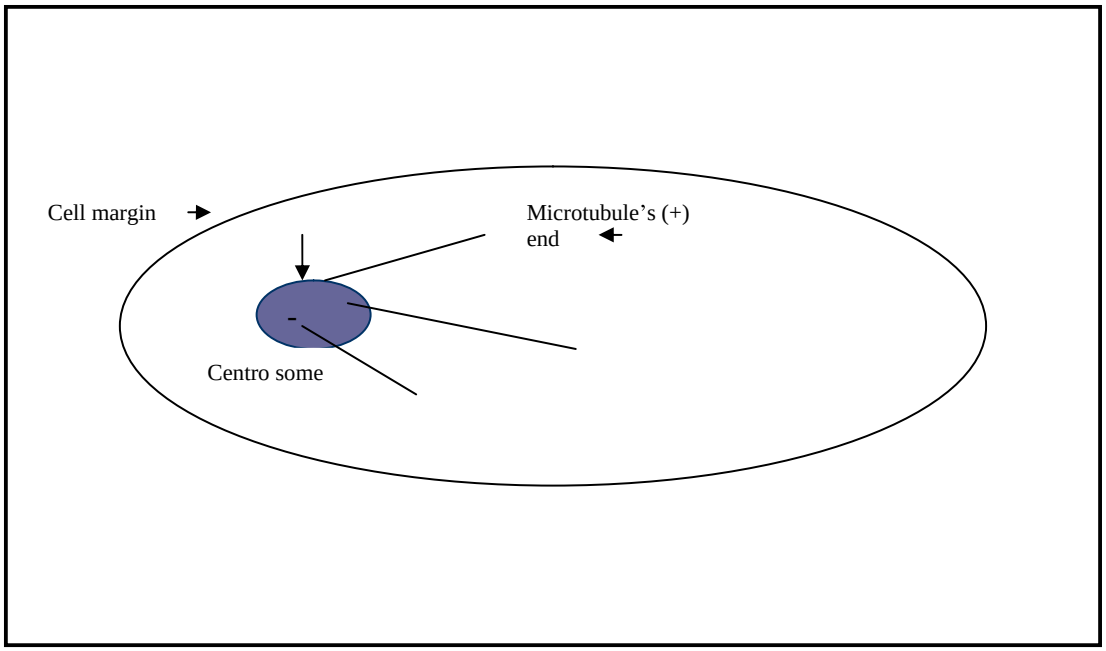

Figure 1.3: A schematic illustration of microtubules inside the cell. Minus ends of microtubules are usually embedded in the microtubule organization center (MOC) which is often the centrosome, while plus ends grow toward the cell margin and experience dynamic instability.

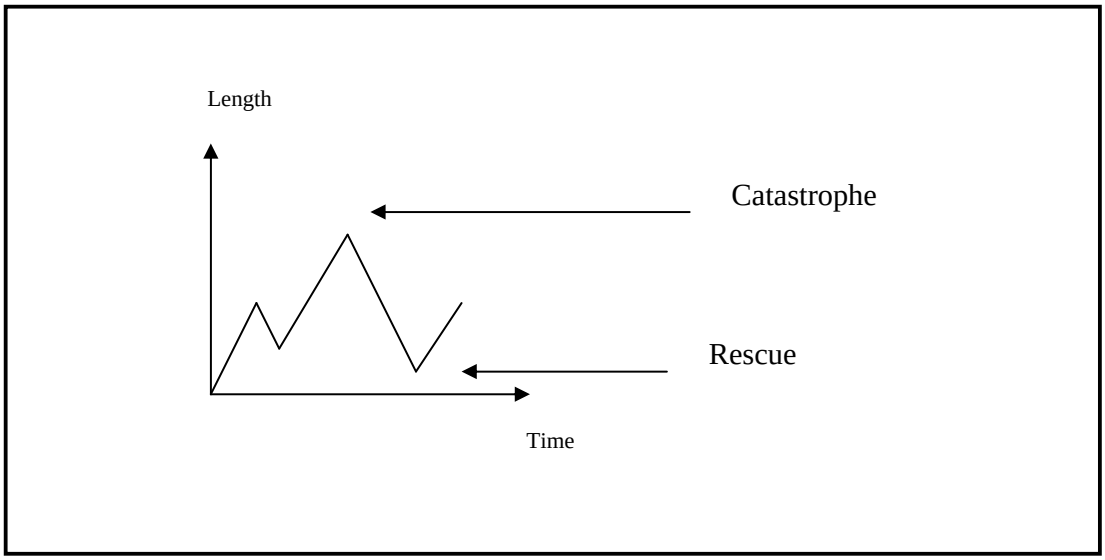

Figure 1.4: A schematic illustration of the life history of a microtubule. A microtubule experiences several phase transitions during its life history. Transition from the growing to the shrinking stage is called catastrophe and transition from the shrinking to the growing stage is called rescue.

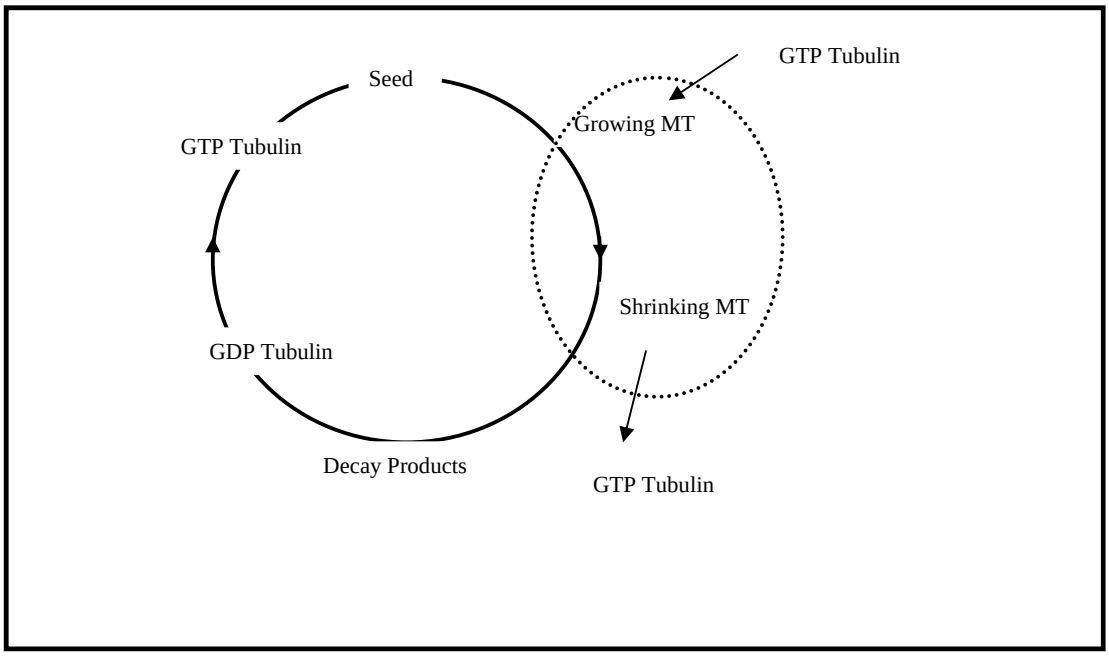

Figure 1.5: A reaction cycle diagram for microtubule assembly. T-tubulin dimers may spontaneously form a seed of microtubules that grow further by adding T-tubulin. A growing microtubule may switch to the shrinking state. D-tubulin dimers (GDP.tubulin) are released in shrinking state. The whole cycle becomes closed by regenerating of T-tubulin from D-tubulin.

Reaction Type	Equation
1- Nucleation	$n_c T$ ----- > $M_g(n_c)$
2- Growth	$M_g(n) + T$ ----- > $M_g(n+1)$
3- Shrinkage	$M_g(n)$ ---- > $M_g(n-1) + T$
4- Catastrophe	$M_g(n)$---- > $M_c(n)$
5- Rescue	$M_c(n)$ ---- > $M_g(n)$
6- Reaction	D + GTP ---- > T+GDP

Figure 1.6: A list of key chemical reactions involved in microtubule assembly. T is GTP-tubulin, D^+ are depolymerization products, D is GDP-tubulin, $M_g(n)$ is a microtubule in the growing state which consist of n tubulin dimers. $M_c(n)$ is a microtubule in the collapsing state and n_c is the size of the critical nucleus in a model with homogeneous nucleation.

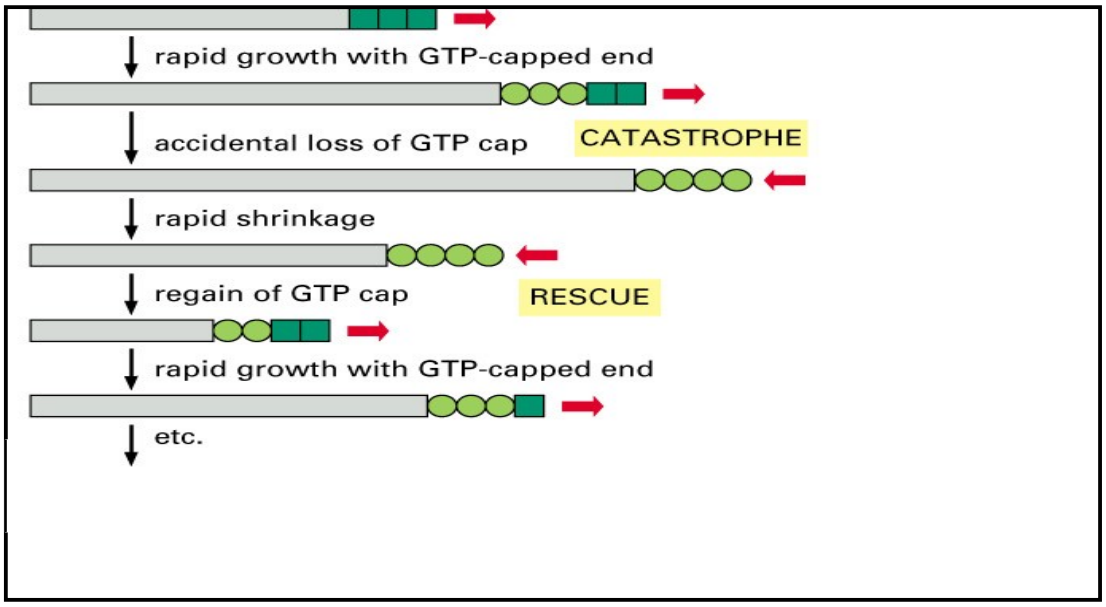

Figure 1.7: T-tubulins (GTP.tubilin) added to the end of a microtubule act as stabilizer. While a microtubule has a GTP cap, it can remain in the growing phase. A microtubule is no longer stable when the GTP cap is lost and in fact hydrolisis of GTP in the GTP. In that moment a microtubule switch to shrinking stage. It may experience rescue and back to growing stage if it gain a new GTP cap.

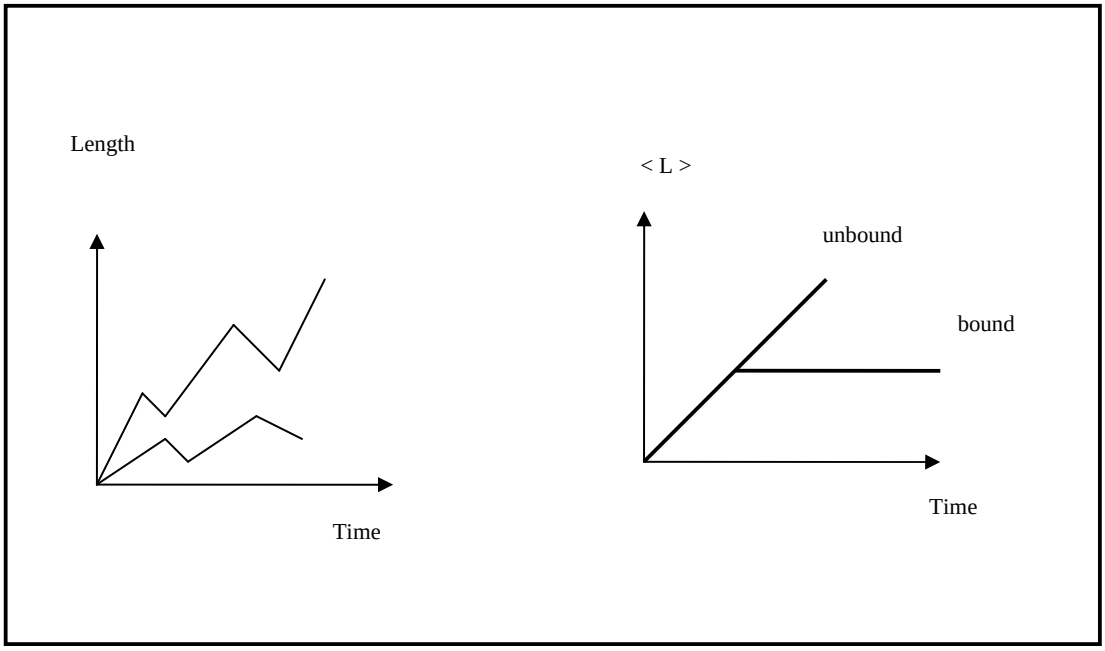

Figure 1.8: Microtubules can have an unbounded length distribution or bound distribution. In the unbound regime, the mean value of the length distribution increases by time, while for a bound regime, the mean value of the length distribution is constant and independent of time.

Chapter 2

Polymerization of Microtubules in the Presence of Substoichiometric Levels of Antimitotic Drugs

2.1 Introduction

This chapter consists of two parts:

- Review of the current mathematical models for polymerization of microtubules by pure T-tubulin.
- Expansion of one of these mathematical models for co-polymerization of microtubules by pure T-tubulin and a T-tubulin- anti-mitotic drug complex.

The first section of this chapter will introduce two well-known mathematical models that express the dynamics of microtubules, developed by Hill (1997) and Freed (2002). The next section will briefly introduce the effects of antimitotic drugs on the polymerization of microtubules. One of these models, the Hill model, will then be modified to include kinetic equations of microtubule dynamics in the presence of low concentrations of antimitotic drugs. Steady state solutions of these kinetic equations will be presented in this section as well. Through the power of numerical calculations, the

behavior of one the biological parameters will be investigated. This chapter will conclude with a comparison of model calculations to experimental data.

2.2 A discrete mathematical model for microtubule assembly dynamics

This section briefly reviews earlier models of dynamic instability. The analysis assumes simple stiff, non-interacting polymers growing in an infinitely homogeneous medium. Consider a situation where a large number of microtubules are present so that the experimenter can measure various associated averaged quantities for an ensemble of microtubules of different lengths. The general equation for the evolution of the probability distribution $P(n,t)$ which characterizes the system in a given state n at a time instant t is:

$$\partial_t P(n,t) = (rate"in") - (rate"out"). \tag{1}$$

Note that the $n = 0$ state is the seed state; it plays an important role in the boundary conditions.

Based on this perspective, two models have been presented for the dynamics of microtubules: Hill's model and Freed's model. The following sections review these two models.

2.2.1 Hill model

Studies by Hill presented some introductory analytical results relating to the existence of two different "phases" on the end of a microtubule. A kinetic scheme for one end of a very long two- phase polymer, or for a two-phase polymer aggregating on a nucleated site, is presented in Fig.2. 1. The mathematical model for the dynamics of a two-phase polymer presented by Hill is based on this schematic view.

In this model:

- The variable n counts subunits added to or lost from only one end of the polymer.
- The states in growing phase or shrinking phase have probabilities $P_+(n,t)$ and $P_-(n,t)$, respectively at time t.

- Phase changes (catastrophe and recovery) happen with the frequencies of f_c and f_r, respectively.
- λ and λ' are rate constants. The on (λ) and off (λ') processes are not the inverse of each other. likewise for μ and μ' (on and off rate in the shrinking stage) .

The kinetic equations can be written as:

$$\partial_t P_+(n,t) = \lambda P_+(n-1,t) + \lambda' P_+(n+1,t) + f_r P_-(n,t) - (\lambda + \lambda' + f_c) P_+(n,t), \tag{2a}$$

$$\partial_t P_-(n,t) = \mu P_-(n-1,t) + \mu' P_-(n+1,t) + f_c P_+(n,t) - (\mu + \mu' + f_r) P_-(n,t), \tag{2b}$$

The other needed relations for the analysis are:

$$\partial_t P_+(0,t) = \lambda' P_+(1,t) + \mu' P_-(1,t) - \lambda P_+(0,t), \tag{2c}$$

$$\partial_t P_-(1,t) = \mu' P_-(2,t) + f_c P_+(1,t) - (\mu + \mu' + f_r) P_-(1,t). \tag{2d}$$

In this model whenever:

- $\lambda < \lambda'$ there is a finite attached polymer.
- $\lambda = \lambda'$ the polymer becomes infinitely large.
- $\lambda > \lambda'$ the polymer grows at the rate $p_g = \lambda - \lambda'$.

If we replace λ and λ' with a unidirectional composite $p_g = \lambda - \lambda'$ and μ and replace μ' with composite $-p_s$, the model becomes especially useful because its mathematical properties are simpler.

The steady state solution is achievable in the case $\lambda' \to 0, \mu \to 0, \lambda \to p_g, \mu' \to p_s$. The above equations can be written as:

$$\partial_t P_+(n,t) = p_g P_+(n-1,t) + f_r P_-(n,t) - (p_g + f_c) P_+(n,t), \tag{3a}$$

$$\partial_t P_-(n,t) = p_d P_-(n+1,t) + f_c P_+(n,t) - (p_d + f_r) P_-(n,t), \tag{3b}$$

$$\partial_t P_+(1,t) = p_g P_0(t) + f_r P_-(1,t) - (p_g + f_c) P_+(1,t), \tag{3c}$$

$$\partial_t P_0(t) = -p_g P_0(t) + p_d P_-(1,t). \tag{3d}$$

where p_d is shrinking rate.

By definition, a steady state for microtubule dynamics means time-invariant kinetic parameters, polymer levels and spatial distribution. In the steady state, the left hand side of the above equations vanish. Imposing the normalization condition $\sum_{n=1}^{\infty} P_+(n) + \sum_{n=1}^{\infty} P_-(n) + P_0 = 1$, the steady state solution of the equations is:

$$P_+(n) = x_H^n P_0, \tag{4a}$$

and

$$P_-(n) = x_H^{n-1} y_H P_0, \tag{4b}$$

with

$$P_0 = \frac{1 - x_H}{1 + y_H}, \tag{4c}$$

$$x_H = \frac{p_g(p_d + f_r)}{p_d(p_g + f_c)}, \tag{4d}$$

and

$$y_H = \frac{p_g}{p_d}. \tag{4f}$$

The two-phase model makes it possible to understand qualitatively the total length distribution of microtubules in the steady state. Also, the model can answer questions like how long microtubules can grow well below the critical concentration. The application of analytical steady state solutions to predict some of the biological parameters involved will be discussed elsewhere in this chapter.

2.2.2 Freed model

Freed extended Hill's model for the kinetic of individual microtubule formation [23]. The treatment of nucleation sites and the explicit inclusion of tubulin concentration in which a two-fold infinite set of coupled equations becomes nonlinear contains the major mathematically complicated elements involve in modeling the microtubule dynamics.

The related equations are expressed as follows:

$$\partial_t P_+(n,t) = \rho p_g P_+(n-1,t) + f_r P_-(n,t) - (\rho p_g + f_c) P_+(n,t), \tag{5a}$$

$$\partial_t P_-(n,t) = p_d P_-(n+1,t) + f_c P_+(n,t) - (p_d + f_r) P_-(n,t), \tag{5b}$$

and

$$\partial_t P_+(1,t) = p_n \rho N + f_r P_-(1,t) - (p_g \rho + f_c) P_+(1,t), \tag{5c}$$

$$\rho_0 = \rho + Q_+ + Q_-, \tag{5d}$$

where

$$Q_{+/-} = \sum_{n=1}^{\infty} n P_{+/-}(n,t). \tag{5e}$$

Furthermore

$$N_0 = N + P_+ + P_-, \tag{5f}$$

where

$$P_{+/-} = \sum_{n=1}^{\infty} P_{+/-}(n,t). \tag{5g}$$

The steady state solution of this system of kinetic equations is given by [23]:

$$P_+ = \frac{p_n N_0 (f_r + p_d)}{D}, \tag{6a}$$

$$P_- = \frac{p_n N_0 (f_c + p_g \rho)}{D}, \tag{6b}$$

and

$$P_-(1) = \beta' = \frac{p_n \rho_0 (p_d f_c - p_g f_r)}{(p_d D)}, \tag{6c}$$

where

$$D = p_n p_g \rho^2 + (p_d p_n - p_g f_r)\rho + (p_d f_c + p_n f_r). \tag{6d}$$

where p_n is the rate of binding a tubulin subunits with a free nucleation site.

With the help of the generation function method, the analytical expression can be calculated as follows:

$$P_+(n) = (a'c')^{(n-1)/2}[(f' + \beta' d')U_{n-1}(\lambda') - (a'c')^{-1/2}a'f'U_{n-2}(\lambda')] \quad (7a),$$

and

$$P_-(n) = (a'c')^{(n-1)/2}[\beta' U_{n-1}(\lambda') - (a'c')^{-1/2}(b'f' - c'\beta')U_{n-2}(\lambda')] \quad (7b),$$

where

$$a' = \frac{(p_d + f_r)}{p_d} \quad (7c),$$

$$b' = \frac{-f_c}{p_d} \quad (7d),$$

$$c' = \frac{p_g\rho}{(p_g\rho + f_c)} \quad (7e),$$

$$d' = \frac{f_r}{(p_g\rho + f_c)} \quad (7f),$$

$$f' = \frac{p_n\rho N}{(p_g\rho + f_c)} \quad (7g),$$

$$\lambda' = \frac{(a' + b'd' + c')}{(2(a'c')^{1/2})} \quad (7h).$$

and $U_n(\lambda')$ is Chebyshev's polynomial of the second kind given by:

$$U_n(\lambda') = \frac{sin[(n+1)arccos\lambda']}{(1-\lambda'^2)^{1/2}}. \quad (7i).$$

In these equations, ρ_0 is the initial concentration of tubulin subunits and ρ is the corresponding instantaneous concentration at time t. Similarly N_0 and N are the initial and instantaneous numbers of free nucleating sites respectively. Binding of a tubulin subunit with a free nucleating site takes place at a rate p_n.

In this dissertation the effect of tubulin concentration is neglected and modification of kinetic equations for the co-polymerization process are modified based on the Hill model. In the last chapter of this dissertation, the possibility of expanding the Freed model for the co-polymerization process will be discussed. Before focusing on the mathematical perspective of co-polymerization of microtubules in the presence of antimitotic agents, the effects of antimitotic drugs on microtubule dynamics is presented.

2.3 Antimitotic drugs

A large number of chemically diverse substances bind to soluble tubulin or directly to tubulin in microtubules. Most of these compounds are antimitotic agents which inhibit cell proliferation by acting on the polymerization dynamics of spindle microtubules, which are essential to proper spindle function. How each drug targets the microtubule polymer mass and dynamics is complex. There have been numerous reviews of microtubule polymerization and drug interaction from a physiochemical perspective in the last decade [29]-[35].

Several key points in the study of antimitotic drugs are expressed below:

- The effects of antimitotic drugs on the polymerization of microtubules in vitro vs. in vivo.
- The effects of antimitotic drugs on the polymerization of microtubules in a dose-dependent manner.
- Specific drug mechanisms.

Antimitotic drugs destabilize polymerization in the cell (in vivo) differently than in vitro due to several factors present in the cell: enzymes, stabilizing proteins (MAPs) and dynamic regulatory proteins. The exact mode of drug activity in vivo is thus uncertain [36]. A central assumption in this presentation is that these drugs preserve their in vitro molecular structure while interacting with the microtubule body to disrupt dynamics in vivo [37], [38], [39].

Drugs can behave differently at low doses, called substoichiometric levels, compared to high or stoichiometric levels. In fact, drugs that increase or decrease microtubule polymerization at high concentrations powerfully suppress microtubule dynamics at 10-100-fold lower concentrations. In other

words, substoichiometric levels of antimitotic drugs kinetically stabilize the microtubule. Stabilization can occur at both microtubule ends, at one end, or some combination thereof in a drug concentration-dependent manner. This chapter focuses on how low concentrations of drugs effect the plus ends of microtubules.

Antimitotic drugs can be classified into various groups based upon their site and type of binding and their mode of interaction. We will focus on a tubulin-centered vision of drug action. There are three general classes of drug binding sites on tubulin: the colchicine binding site, the vinca alkaloid site and the taxol site [39].

This chapter continues with a discussion of low concentrations of colchicine, while the next chapter covers high concentrations. Colchicine has been chosen for this study because its irreversible binding to tubulin simplifies the model equations.

2.4 Extended Hill's model in the presence of low concentrations of colchicine

In this section, the preliminary assumptions for extending the mathematical model for dynamics of microtubules in the presence of low concentrations of colchicine is discussed. Kinetic equations are built up and steady state solutions are calculated.

It has been observed that each tubulin dimer has binding sites for a variety of biologically important ligand-like therapeutic drugs [39]. One of these mitotic drugs is colchicine (COL). Colchicine binds irreversibly to the tubulin dimer at a site near the intra-dimer [40]. Colchicine is well known as a cytostatic agent because of its effective inhibition of microtubule polymerization [40].

Reported data suggests that the T-tubulin-colchicine complex (TTC) suppresses microtubule growth and actives the weak GTPase activity in the dimer [36]. This effect is long-lasting due to irreversible binding of colchicine to tubulin [42].

Since colchicine opposes the typical effect of GTP hydrolysis, the number of catastrophe events decreases sharply in the population of microtubules with colchicine binding. As a good approximation, colchicine acts as a catastrophe-suppressing drug in vitro. Kinetically stabilizing and capping

the microtubules ends occurs in the low concentrations of colchicine [42].

By adding a specific amount of colchicine and assuming immediate binding, two species of subunits exist in the solution; T-tubulin-colchicine subunits and T-tubulin subunits (TT). These two species of subunits have the ability to co-assemble into a microtubule. Two groups of polymerized microtubules can exist in this case.

The first group are microtubules with T-tubulin-colchicine tips. They are very stable, remain in the growing stage, and do not experience catastrophe. The probability of growth for a microtubule with TTC tip, with length n at time t, is expressed by $\Pi(n,t)$.

The second group consists of microtubules with T-tubulin tips. Microtubules in the second group can experience dynamic instability and can switch between the growing and shrinking stages. $P_+(n,t)$ and $P_-(n,t)$ are the probabilities of growing and shrinking of a microtubule in this group (with length n at time t). A schematic view of two species of subunits and two groups of polymerized microtubules is shown in Fig.2.2.

The assembly rate of a microtubule depends on the concentration of free subunits plus the interaction between a microtubule tip and the subunits. These interactions are not accounted for in this work. Here, it is assumed that the two species of subunits have different concentrations in the solution. This implies that each microtubule has the ability to grow with two different velocities. We assume a low concentration of T-tubulin-colchicine subunits so as to be consistent with experimental data on stabilized microtubules and to include the hypothesis of capping the microtubules ends. In this study p_c, the assembly rate by addition of T-tubulin-colchicine subunits at the end of a microtubule is smaller than p_g , the assembly rate by addition of T-tubulin subunits. For a microtubule with a tubulin tip, p_d is the shrinking velocity, f_c is frequency of catastrophe and f_r is the frequency of rescue. A schematic illustration of the co-polymerization of a microtubule is shown in Fig.2. 3.

Polymerization dynamics with two species of subunits is known as co-polymerization dynamics and can be expressed by a modified Hill model.

The kinetic equations of two groups of microtubules can be expressed by the following equations:

$$\frac{\mathrm{d}P_+(n,t)}{\mathrm{d}t} = p_g\left[P_+(n-1,t)+\Pi(n-1,t)\right]+f_rP_-(n,t) \\ -(p_g+p_c+f_c)P_+(n,t); n>2, \tag{8a}$$

$$\frac{\mathrm{d}P_-(n,t)}{\mathrm{d}t} = p_d P_-(n+1,t) + f_c P_+(n,t) - (p_d + f_r) P_-(n,t); n > 1, \quad (8b)$$

$$\frac{\mathrm{d}P_+(1,t)}{\mathrm{d}t} = p_g P_0(t) + f_r P_-(1,t) - (p_g + p_c + f_c) P_+(1,t), \quad (8c)$$

$$\frac{\mathrm{d}P_0(t)}{\mathrm{d}t} = -(p_g + p_c) P_0(t) + p_d P_-(1,t), \quad (8d)$$

$$\frac{\mathrm{d}\Pi(n,t)}{\mathrm{d}t} = p_c \left[P_+(n-1,t) + \Pi(n-1,t)\right] - (p_g + p_c)\Pi(n,t); n > 2, \quad (8e)$$

$$\frac{\mathrm{d}\Pi(1,t)}{\mathrm{d}t} = p_c P_0(t) - (p_g + p_c)\Pi(1,t). \quad (8f)$$

The steady state solutions for these equations are:

$$P_+(n) = x(x+z)^{n-1} P_0, \quad (9a)$$

$$P_-(n) = y(x+z)^{n-1} P_0, \quad (9b)$$

$$\Pi(n) = z(x+z)^{n-1} P_0. \quad (9c)$$

where

$$P_0 = \frac{1-x-z}{1+y}. \quad (10)$$

with

$$x = \frac{p_g(p_d + f_r) + p_c f_r}{p_d(p_g + f_c) + p_c p_d}, \quad (11a)$$

$$y = \frac{p_g + p_c}{p_d}, \quad (11b)$$

$$z = \frac{p_c}{p_c + p_g}. \quad (11c)$$

When p_c tends to zero, these solutions will converge to the steady state solutions of the Hill model [17, 44].

2.5 Evolution of free T-tubulin concentration

To find a bridge between the mathematical equations and experimental results, one may analytically or numerically calculate one of the measurable biological parameters. Steady state polymer mass has been measured experimentally [43]. This quantity can also be calculated mathematically with the help of the present model. In order to reach to this goal, complementary equations determine free T-tubulin concentration and, indirectly, polymer mass in the steady state. The procedure is as follows:

Dynamic equations (8a-8f above) are completed by adding the time evolution equations for T-tubulin concentration and T-tubulin-colchicine concentration in a regeneration system.

Microtubules with T-tubulin tips which can switch to the shrinking stage are the only group of microtubules involved in the polymerization cycle. A schematic view of the polymerization cycle is shown in Fig.2. 4.

The kinetic equations for tubulin concentrations are:

$$\frac{\mathrm{d}C_T^*}{\mathrm{d}t} = -p_g\gamma\left[\sum_{n=1}^{\infty}\left(P_+(n,t)+\Pi(n,t)\right)\right]+\alpha C_d, \tag{12a}$$

$$\frac{\mathrm{d}C_T^{**}}{\mathrm{d}t} = -p_c\gamma\left[\sum_{n=1}^{\infty}\left(P_+(n,t)+\Pi(n,t)\right)\right], \tag{12b}$$

and

$$\frac{\mathrm{d}C_d}{\mathrm{d}t} = p_d\gamma\sum_{n=1}^{\infty}P_-(n,t)-\alpha C_d. \tag{12c}$$

In the above equations, C_T^* is the T-tubulin concentration without drug bonding, C_T^{**} is the concentration of T-tubulin with drug bonding, C_d is the D-tubulin concentration, α is the regeneration rate which can be assumed to be approximately constant in the presence of high concentration of free GTP [13] and γ is the length factor describing the number of tubulin dimer that are incorporated in a unit length of microtubules.

We also have the conservation of tubulin subunits which is expressed below, with C_0 the overall concentration of tubulin subunits.

$$C_T^*+C_T^{**}+C_d+\gamma\left[\sum_{n=1}^{\infty}nP_+(n,t)+\sum_{n=1}^{\infty}n\Pi(n,t)\right]=C_0. \tag{13}$$

The total T-tubulin concentration is:

$$C_T^* + C_T^{**} = C_T. \tag{14}$$

The dynamics of total T-tubulin concentration can be obtained by eliminating C_d from Eq.(12a) and adding equations (12a) and (12b). The time variation of the T-tubulin concentration can then be expressed by following equation:

$$\frac{\mathrm{d}C_T}{\mathrm{d}t} = -(p_g + p_c)\gamma \left[\sum_{n=1}^{\infty}(P_+(n,t) + \Pi(n,t))\right]$$
$$-\alpha\gamma \left[\sum_{n=1}^{\infty} n(P_+(n,t) + \Pi(n,t))\right] + \alpha(C_0 - C_T). \tag{15}$$

As we see, microtubules with drug bonding do not affect the polymerization cycle, but are involved in the dynamics of total T-tubulin concentration.

In the steady state the left hand side of Eq. (15) vanishes and the stationary total T-tubulin concentration C_T^0 can be determined by the nonlinear self-consistent equation:

$$\alpha(C_0 - C_T^0) = (p_g + p_c)\gamma P_0(\frac{K}{1-K}) + \alpha\gamma P_0 \frac{K}{(1-K)^2}. \tag{16}$$

.

where $K = x + z$.

In our calculations, we assumed that the frequency of rescue was negligible for plus ends.

2.6 Behavior of total T-tubulin concentration in the steady state

One can discuss the behavior of total T-tubulin concentration in the steady state analytically when the frequency of catastrophe is linearly dependent on tubulin concentration and numerically when the frequency of catastrophe has an exponential dependence with pure T-tubulin concentration.

2.6.1 Numerical calculation

- Growth velocity and catastrophe rate

In a recent experiment with the high tubulin-t concentration, the growing velocity was independent of C_T, so we focus on a high range of T-tubulin concentration and assume a constant growing velocity. It means that p_g, p_c and p_d are constant [45].

In this stage, the total free T-tubulin concentration as a function of regeneration rate in the presence and absence of colchicine can be calculated via numerical analysis. Our calculations focus on the following points:

- The order of magnitude of p_g and p_d was obtained from Houchmandzadeh [13]. Vandecandlaere et al. [46] referred to low concentrations of T-tubulin-colchicine as accruing when the ratio of T-tubulin-colchicine to T-tubulin is between 0.02 and 0.05. As explained in section 2, since growth rates are proportional to the concentration of free subunits, the ratio of p_g to p_c should be in the this range as well, to fulfill the requirement of a low concentration of T-tubulin-colchicine. The ratio of T-tubulin-colchicine to T-tubulin is 0.03 in our calculation, Fig.2.5.

- The exponential dependence of the catastrophe frequency.

- The amount of free total T-tubulin in the steady state as a function of the regeneration factor for two different sets of number of subunits in unit of length γ calculated Fig.2.6.

- The amount of free total T-tubulin concentration in the steady state as a function of regeneration rate for two sets of different catastrophe frequencies calculated Fig.2.7.

- Calculations centered on total free T-tubulin concentration in the steady state as a function of regeneration rate for a set of parameters in the presence and absence of a low concentration of colchicine. Experimental data were compared with predictions, Fig.2.5.

2.6.2 Numerical results

Our numerical results are as follows:

- The effect of low concentrations of tubulin-colchicine complex in vitro and at the steady state has been studied experimentally by Panda et al. [43] also by Vandecandlaere et al. [46]. Panda's data shows that substoichiometric or low concentration of tubulin-colchicine complex strongly suppress the catastrophe frequency without reducing the polymer mass.

  The behavior of total free T-tubulin concentration in the steady state and in the presence of low concentrations of colchicine has been investigated in this thesis. The simulation displayed in Fig.2.5 indicates that the amount of free T- tubulin concentrations and therefore polymer mass does not significantly change in the presence of low concentration of T-tubulin-colchicine. This strongly supports the idea that colchicine has the ability to stabilize microtubules by regulating their dynamics. As can be seen from the Fig.2.5 this model is in qualitative agreement with results reported by Panda et al. [43].

  The very small change in the free tubulin concentration in the absence and presence of low concentrations of colchicine can be ignored due to the results in [43]. Significant change occurs when polymer mass changes by a factor of 2 or 3 [47] .

  The boundary conditions we applied to our mathematical equations that microtubules with T-Tubulin-colchicine tips cannot experience catastrophe at all might also be the cause of the small difference between our numerical calculations and experimental results.

- The free total T-tubulin concentration is a function of the regeneration factor for small α and independent of the regeneration factor when α is large enough, the reason being that a large regeneration rate causes the D-tubulin population to be constantly converted to T-tubulin.

- The amount of total free T-tubulin concentration is also dependent on the subunits length, γ, as we see in Fig. 2.6 (by increasing γ the amount of free T-tubulin concentration is decreased).

- The total polymer mass or total free T-tubulin concentration in the steady state is directly proportional to the frequency of catastrophe of microtubule with pure tubulin tip as we can see in Fig.2.7. By increasing the frequency of catastrophe in the steady state, the total T-tubulin concentration increases as well.

2.6.3 Analytical calculation

In this section a linear C_T dependence is considered for the frequency of catastrophe:

$$f_c(c_T) = f * (c_u - c_T). \tag{11}$$

with appropriate constant $c_u > c_t$.

If the linear dependence of the catastrophe rate in Eq.(11) is chosen for the special case $c_u = c_0$, the explicit expression for the behavior of T-tubulin concentration in the steady state as a function of regeneration rate can be calculated as below:

$$f_c^0(c_T) = f(c_0 - c_T^0). \tag{14}$$

By substituting this equation in Eq.(88) and after some calculation and simplification we obtain:

$$c_0 - c_t^0 = \frac{\gamma P_0}{f_c^2}[\frac{f_c}{\alpha}\frac{\gamma P_0 (p_g + p_c)^3}{p_g} + \frac{f_c^2}{\alpha}\frac{p_c(p_c + p_g)}{p_g}$$
$$\frac{(p_g + p_c)^4}{p_g^2} + \frac{f_c(p_g + p_c)^3}{p_g^2} + \frac{f_c p_c (p_g + p_c)^2}{p_g^2} + \frac{f_c^2 p_c (p_g + p_c)}{p_g^2}]$$

In the limit $\alpha \gg f^2$, we see that the above equation is independent of α. When the frequency of catastrophe has a decaying exponential behavior independent of T-tubulin concentration, regeneration rate can not be expressed through analytical calculations.

2.7 Conclusions

In this chapter, we have examined the mechanism of regulatory drug molecules that stabilize microtubule dynamics and concepts of copolymerization of microtubules expressed through the mathematical perspective.

It seems reasonable to conclude based on that colchicine suppresses the dynamics of spindle microtubules rather than de-polymerizing the microtubules at low concentration (almost hundred times less than concentration of pure T-tubulin) in vitro.

According to the view developed in this work, in the presence of low concentrations of colchicine, a microtubule can potentially grow at two different growth rates related to two different concentrations of subunits in the solution. The concentration of TTC subunits is less than TT subunits. Therefore, the average growth rate which decreases can be interpreted as a regulatory factor. Also, the ability of TTC to stabilize microtubule ends is another factor that regulates and suppresses dynamic instability. These two factors are reflected in the kinetic equations and lead to results similar to those reported experimentally.

The emphasis on blocking the frequency of catastrophe is a simplified assumption at this stage of modeling and is a point of discrepancy between this mathematical model and biological experiments. Expanding this mathematical treatment to a more complex model will be discussed in the next chapter.

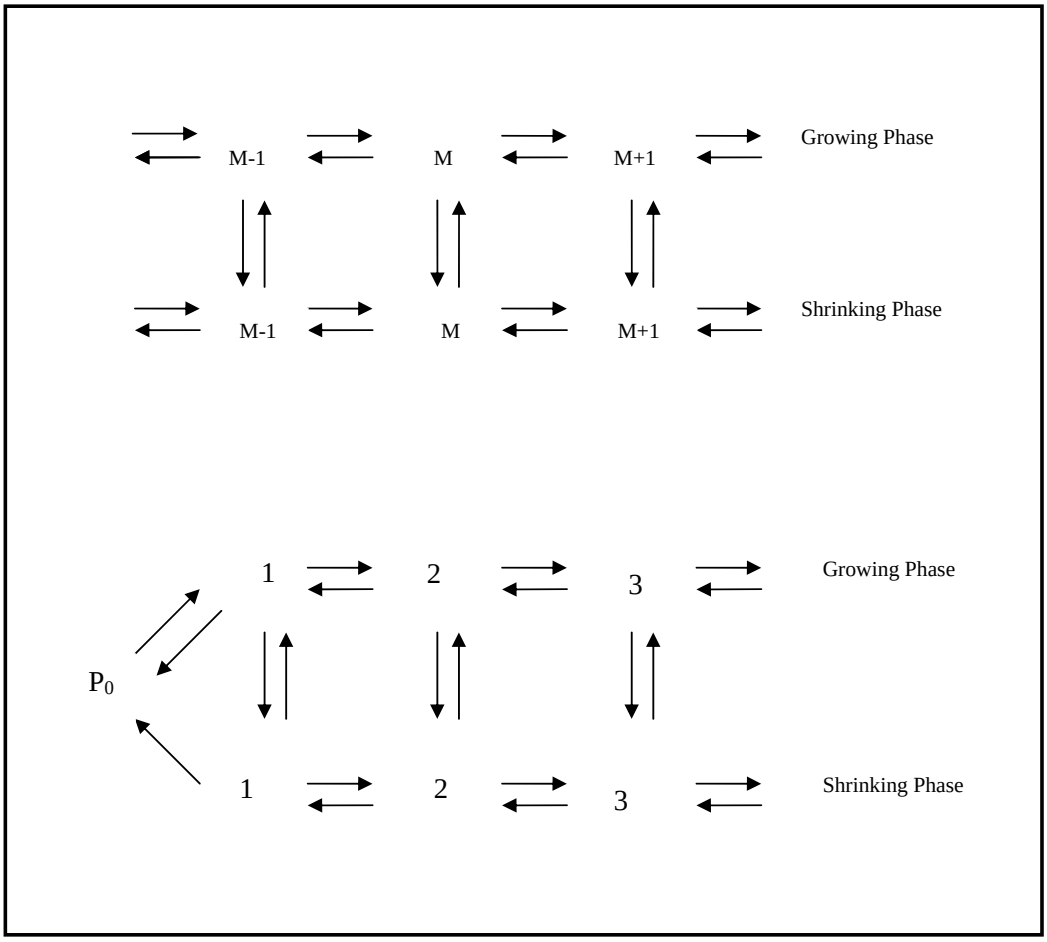

Figure 2.1: Kinetics of the two-phase polymer

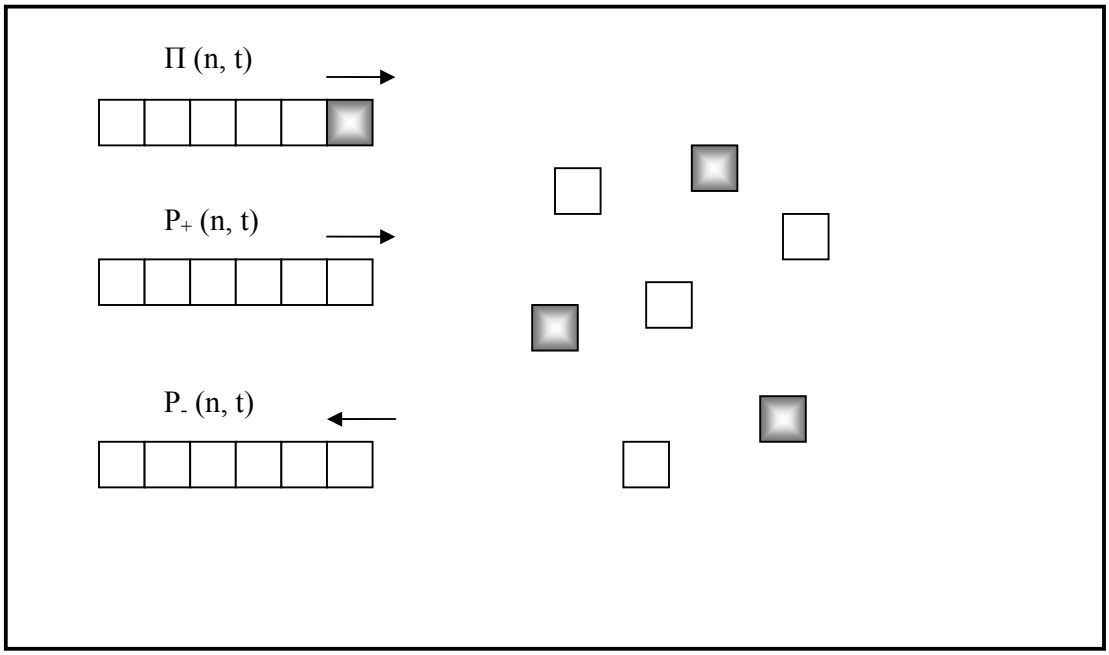

Figure 2.2: Boxes with shadow indicate T-tubulin-colchicine subunits and colorless boxes indicate T-tubulin subunits in this view. Two groups of polymerized microtubules, with TTC tips and with TT tips are also shown.

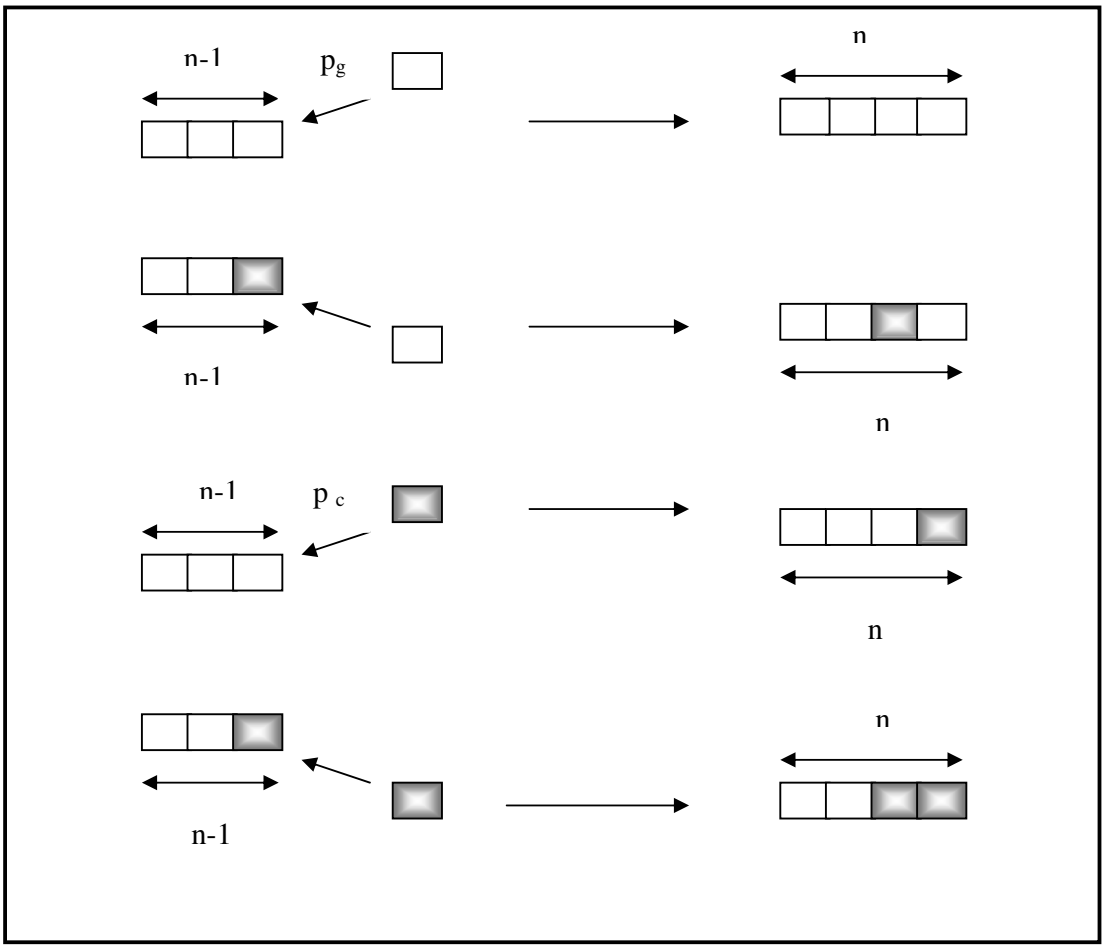

Figure 2.3: The concept of co-polymerization dynamics is expressed in this figure. Because two sets of free subunits exist with different concentrations, microtubules can be copolymerized with two different assembly rates p_g and p_c.

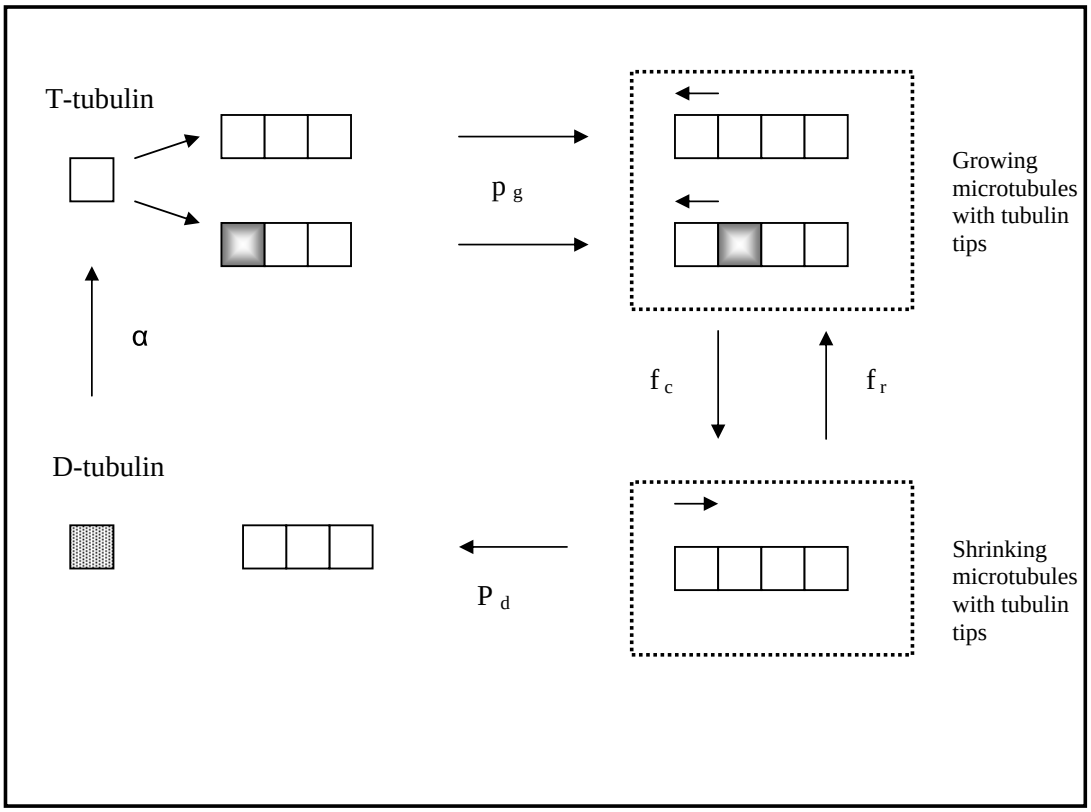

Figure 2.4: Microtubules with TTC tips remain in the growing stage while other microtubules with TT tips are reduced in size with frequency of catastrophe f_c or rescued at frequency f_r. Shrinking velocity is p_d. During the shrinking stage D-tubulin is released into the solution. Regeneration occurs in this system at rate α.

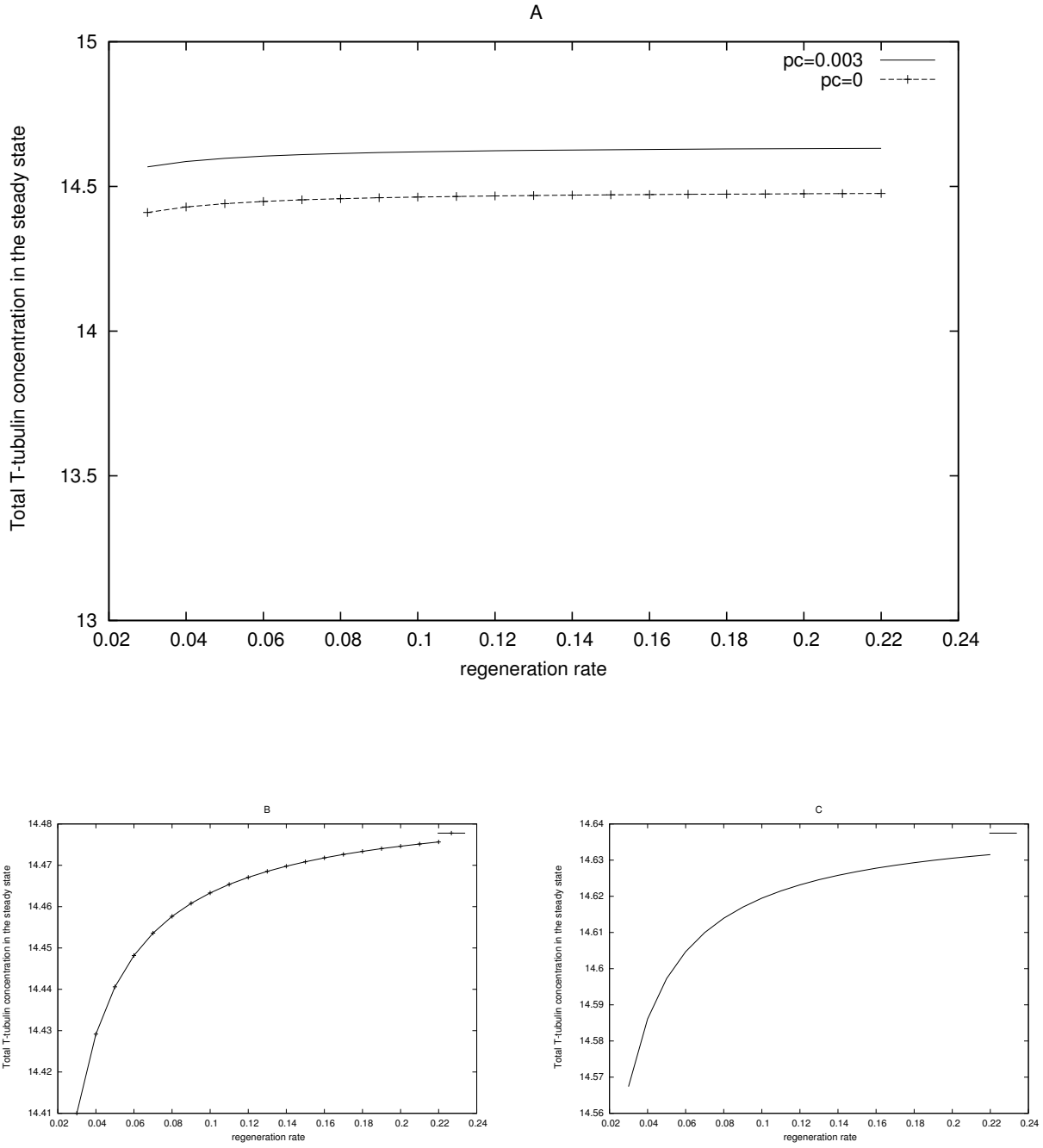

Figure 2.5: (A) indicates the concentration of free total T-tubulin concentration in the presence of colchicine (the dashed line) and in the absence of colchicine (the solid line). In (B) and (C) the dependency of free total T-tubulin concentration for small regeneration rate α is shown. The parameters are: $C_0 = 120$, $p_g = 0.1$, $p_d = 0.4$, $p_c = 0.003$, $f = 0.1$, $C_f = 3$, $\gamma = 1$ Concentrations are in μM and velocities are in $\mu M/second$.

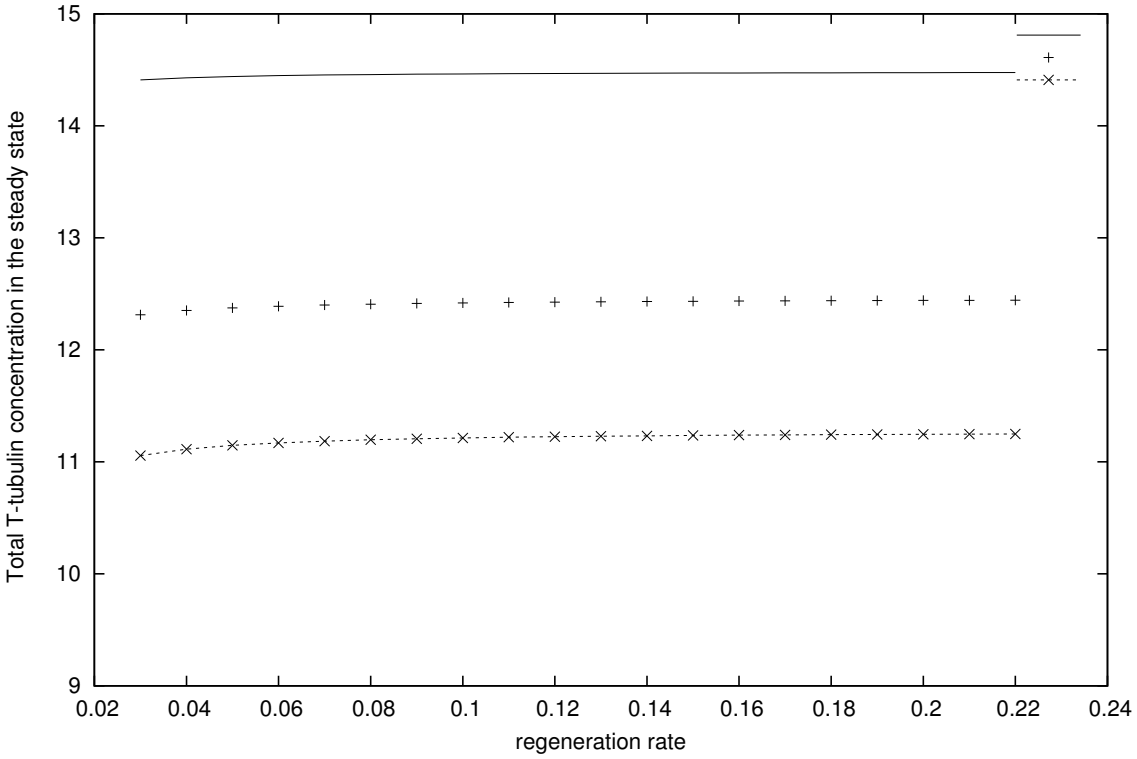

Figure 2.6: The concentration of free total T-tubulin in the steady state as a function of regeneration rate is presented. The parameters are: $C_0 = 120$, $p_g = 0.1$, $p_d = 0.4$, $p_c = 0.003$, $f = 0.1$, $C_f = 3$. and solid line $\gamma = 1$, point line $\gamma = 2$ and line and point $\gamma = 3$.

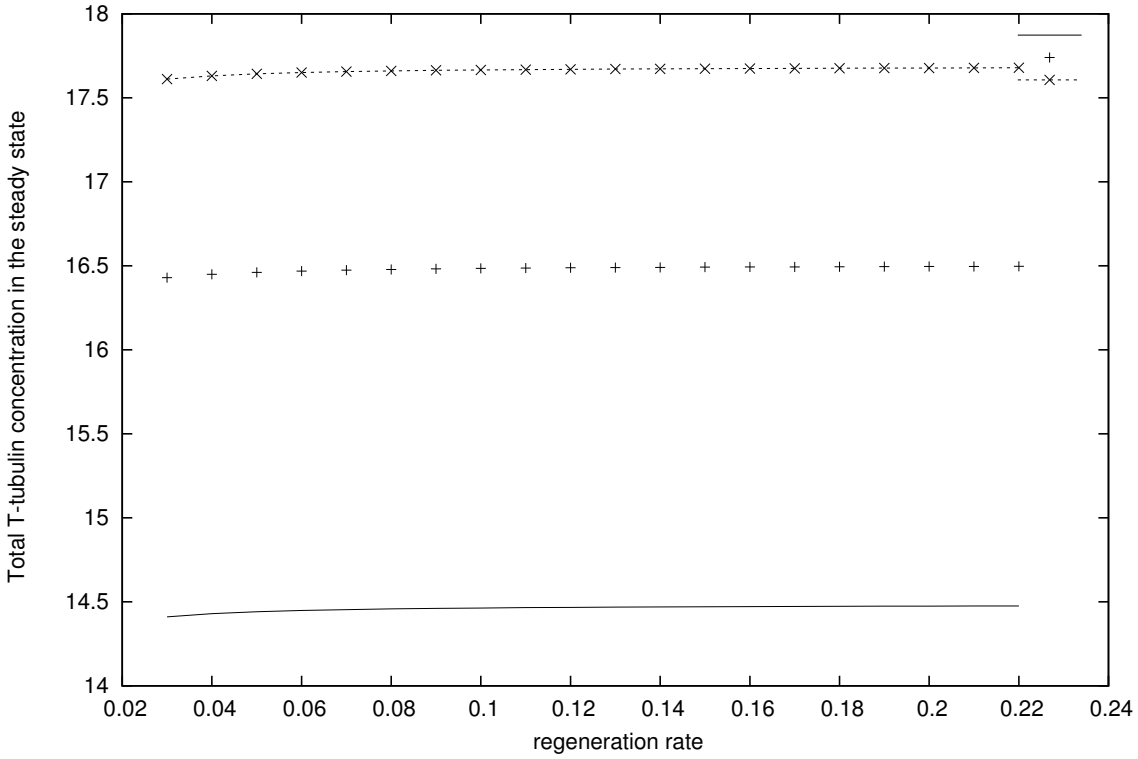

Figure 2.7: The concentration of free total T-tubulin in the steady state as a function of regeneration rate is presented. The parameters are: $C_0 = 120$, $p_g = 0.1$, $p_d = 0.4$, $p_c = 0.003$, $\gamma = 1$, $C_f = 3$. and solid line $f = 0.1$, point line $f = 0.2$ and line and point $f = 0.3$.

Chapter 3

Polymerization of Microtubules in the Presence of Suprastoichiometric Levels of Antimitotic Drugs

3.1 Introduction

The previous chapter constructed a mathematical model to express the polymerization of microtubules in the presence of low concentrations of colchicine. The behavior of total free T-tubulin concentration in the microtubule steady state and in the presence of low concentrations of one of the antimitotic drugs, colchicine, was studied through a mathematical model and with the help of numerical calculations. This phenomenon is known as the substoichiometric effect. An excess of GTP (guanosine triphosphate) available in the solution was assumed in that model. Also, it was assumed the D-tubulin in the solution would exchange its unit of GDP (guanosine diphosphate) with a unit of GTP. It was also assumed that microtubules with T-tubulin-colchicine (TTC) tips could not experience catastrophe.This phenomenon is known as substoichiometric effect.

With suprastoichiometric, high levels of anti-mitotic drugs, colchicine and other antimitotic drugs do not block the frequency of catastrophe. In high concentrations, antimitotic drugs affect all of the dynamic parameters. In this chapter, in order to reach a more realistic model in this level, it was assumed

that even microtubules with drug-tubulin tips experience catastrophe.

Constructing a set of kinetic equations in the suprastoichiometric levels and explaining the structure of these equations are the main part of this chapter. The possibility of having an analytic steady state solution will be investigated also.

The final section will provide numerical calculations on total free T-tubulin concentration in the steady state in a regeneration system.

3.2 Mathematical model

To set the scene, we briefly survey some assumptions and relevant prior work. Our initial investigation began with the one of the simplest models used to express the co-polymerization dynamics with a number of assumptions:

- A microtubule is a one-dimensional polymer [48] and the interaction between a microtubule tip and the incoming subunits was not considered.
- Microtubules with T-tubulin-colchicine tips do not shrink.

With these assumptions, the behavior of the free T-tubulin concentration in the steady state and in the presence of colchicine was investigated. Results indicated that in the presence of a low concentration of T-tubulin-colchicine subunits, the polymer mass in the steady state stays almost constant compared to the case where there is no colchicine in the solution.

The mathematical model is developed further in this chapter by assuming that microtubules with TTC tips can experience catastrophe as well. The number of catastrophe events for these microtubules is smaller than those for microtubules with T-tubulin tips. It is also assumed that microtubules in the shrinking stage cannot be rescued.

As before, by adding a specific amount of colchicine and assuming immediate binding, two species of subunits will exist in the solution, T-tubulin-colchicine subunits (TTC) and T-tubulin subunits (TT). These two species of subunits have the ability to co-assemble into a microtubule. Two sets of polymerized microtubules can exist in this case:

- The first group are microtubules with T-tubulin-colchicine tips. The probabilities of growing and shrinking a microtubule with TTC tip,

with length n at time t, are expressed by $\Pi_+(n,t)$ and $\Pi_-(n,t)$ respectively.

- The second group consists of microtubules with T-tubulin tips. Microtubules in the second group can experience dynamic instability and can switch between the growing and shrinking stage as well. $P_+(n,t)$ and $P_-(n,t)$ are the probabilities of growing and shrinking a microtubule in this group, (with length n at time t).

A schematic view of two species of subunits and two groups of polymerized microtubules is shown in Fig. 3.1.

Growing microtubules have the ability to grow with assembly rate p_g or p_c. Microtubules with TT tips have frequency of catastrophe f_c and shrinking velocity p_d, while microtubules with TTC tips have frequency of catastrophe f_c' and shrinking velocity p_m.

The dynamic parameters will be chosen based on experimental data.

With these basic assumptions, in the following section we will construct the kinetic equations for an ensemble of microtubules with two sets of dynamic parameters for groups of microtubules with and without drug tips.

3.3 Dynamic equations

As before, a very long two-phase polymer grows from one end is considered for this part of modeling. Unlike the previous chapter, the total vacant sites in the lattice Q_0 can be produced by shrinking microtubules with and without a drug tip with the length one (1) at time t.

The time evolution at the boundary is:

$$\frac{\mathrm{d}Q_0(t)}{\mathrm{d}t} = -(p_g + p_c)Q_0(t) + p_d P_-(1,t) + p_m \Pi_-(1,t), \tag{1}$$

Some of the vacant sites can be created by shrinking microtubules with TT tips and length one. This group of vacant sites is called P_0. The rest of vacant sites Π_0 can be created by shrinking microtubules with TTC tips and length one. The above equation can be split into two parts and rewritten as:

$$\frac{\mathrm{d}P_0(t)}{\mathrm{d}t} = -(p_g + p_c)P_0(t) + p_d P_-(1,t), \tag{2}$$

and

$$\frac{\mathrm{d}\Pi_0(t)}{\mathrm{d}t} = -(p_g + p_c)\Pi_0(t) + p_m\Pi_-(1,t), \tag{3}$$

when $Q_0 = P_0 + \Pi_0$.

In the steady state, the left hand sides of equations 2 and 3 vanish. The solution for $P_-(1)$ and $\Pi_-(1)$ are:

$$P_-(1) = XP_0, \tag{4}$$

and

$$\Pi_-(1) = Y\Pi_0, \tag{5}$$

where

$$X = \frac{p_g + p_c}{p_d}, \tag{6}$$

and

$$Y = \frac{p_g + p_c}{p_m}. \tag{7}$$

Let us pause here to introduce a bio-ratio parameter which can be very helpful to simplify calculations. The ratio of P_0 over Π_0 is an integer. Therefore, we can write:

$$\Pi_0 = \theta P_0. \tag{8}$$

We assume that θ is constant, although we can explain that in general it should be a function of free TTC subunits. If drug-tubulin tips increase the catastrophe frequency, then θ is greater than one; otherwise θ is less than one.

In the next step, kinetic equations for microtubules with the length one are expressed as follows:

$$\frac{\mathrm{d}P_+(1,t)}{\mathrm{d}t} = p_g\left[P_0(t) + \Pi_0(t)\right] - (p_g + p_c + f_c)P_+(1,t), \tag{9}$$

and

$$\frac{\mathrm{d}\Pi(1,t)}{\mathrm{d}t} = p_c\left[P_0(t) + \Pi_0(t)\right] - (p_g + p_c + f_c')\Pi(1,t). \tag{10}$$

The left hand sides of those equations vanish in the steady state and we are left with the following solutions for the steady state.

$$P_+(1) = NP_0, \tag{11}$$

and

$$\Pi_+(1) = N'\Pi_0, \tag{12}$$

where

$$N = C(1+\theta), \tag{13}$$

$$N' = A(1+\theta), \tag{14}$$

$$C = \frac{p_g}{p_g + p_c + f_c}, \tag{15}$$

and

$$A = \frac{p_c}{p_g + p_c + f'_c}. \tag{16}$$

In the next step, we rewriting the equation with length n as:

$$\begin{aligned}\frac{\mathrm{d}P_+(n,t)}{\mathrm{d}t} &= p_g\left[P_+(n-1,t) + \Pi_+(n-1,t)\right] \\ &\quad -(p_g + p_c + f_c)P_+(n,t); n > 2,\end{aligned} \tag{17}$$

and

$$\begin{aligned}\frac{\mathrm{d}\Pi_+(n,t)}{\mathrm{d}t} &= p_c\left[P_+(n-1,t) + \Pi_+(n-1,t)\right] \\ &\quad -(p_g + p_c + f'_c)\Pi_+(n,t); n > 2.\end{aligned} \tag{18}$$

In the steady state:

$$P_+(n) = C(1+\theta)(A+C)^{n-1}P_0, \tag{19}$$

and

$$\Pi_+(n) = A(1+\theta)(A+C)^{n-1}P_0. \tag{20}$$

Since the sum of the probabilities will be used in this chapter several times, below symbols for these sums are expressed:

$$P_+ = \sum_{n=1}^{\infty} P_+(n), \tag{21}$$

$$\Pi_+ = \sum_{n=1}^{\infty} \Pi_+(n), \tag{22}$$

$$P_- = \sum_{n=1}^{\infty} P_-(n), \tag{23}$$

and

$$\Pi_- = \sum_{n=1}^{\infty} \Pi_-(n). \tag{24}$$

By these definitions, P_+ and Π_+ can be directly calculated in this case:

$$P_+ = \frac{(1+\theta)C}{1-(A+C)} P_0, \tag{25}$$

and

$$\Pi_+ = \frac{(1+\theta)A}{1-(A+C)} P_0. \tag{26}$$

In the last step, we write the time evolution equations for shrinking microtubules. Writing the kinetic equation for shrinking microtubules is not as straight forward as in the last chapter.

By assuming that there is one tubulin dimer in the unit of length, a microtubule with the length $n+1$ in the shrinking stage can be reduced to a microtubule with length n. This microtubule may have a TT tip or a TTC tip. We know that the population of total microtubules in the shrinking stage changes. Therefore, we can write the following equation:

$$\begin{aligned} \frac{\mathrm{d}}{\mathrm{d}t}[P_-(n,t) + \Pi_-(n,t)] = {} & p_d P_-(n+1,t) + p_m \Pi_-(n+1,t) \\ & + f_c P_+(n,t) + f_c' \Pi_+(n,t) \\ & - (p_d + p_m)[P_-(n,t) + \Pi_-(n,t)]; n > 1, \end{aligned} \tag{27}$$

At this point we introduce the bio-statistical parameters. We can add these parameters to the equation and rewrite it as:

$$\begin{aligned} \frac{\mathrm{d}}{\mathrm{d}t}[P_-(n,t) + \Pi_-(n,t)] = {} & p_d(\alpha+\beta) P_-(n+1,t) + p_m(\gamma+\zeta) \Pi_-(n+1,t) \\ & + f_c P_+(n,t) + f_c' \Pi_+(n,t) \\ & - (p_d + p_m)[(\alpha+\beta) P_-(n,t) + (\gamma+\zeta) \Pi_-(n,t)]; n > 1, \end{aligned} \tag{28}$$

where $\alpha + \beta = 1$ and $\gamma + \zeta = 1$

With the help of these parameters, we can now express the dynamics of shrinking a co-ploymerized microtubule.

This concept is shown in Fig. 3.2. From this figure, equation (28) can be split into two parts:

$$\frac{\mathrm{d}}{\mathrm{d}t}P_{-}(n,t) = p_d\alpha P_{-}(n+1,t) + p_m\gamma\Pi_{-}(n+1,t)$$
$$+f_c P_{+}(n,t) - (p_d + p_m)[\alpha P_{-}(n,t) + \gamma\Pi_{-}(n,t)]; n > 1, \tag{29}$$

and

$$\frac{\mathrm{d}}{\mathrm{d}t}\Pi_{-}(n,t) = p_d\beta P_{-}(n+1,t) + p_m\zeta\Pi_{-}(n+1,t)$$
$$+f_c' P_{+}(n,t) - (p_d + p_m)[\beta P_{-}(n,t) + \zeta\Pi_{-}(n,t)]; n > 1, \tag{30}$$

As can be seen, the bio-statistical parameters allow us to write the time evolution equations for two categories of shrinking microtubules, with TTC tips and with TT tips. Although the bio-statistical parameters should be indexed by n and be explained that in each rescue event, they can select a different set of parameters, for simplicity of this model, they are considered as constant parameters.

In this section, the kinetic equations for the dynamics of microtubules was constructed. To analyze this model and investigate the steady state polymer mass, two different categories are considered; when the shrinking velocity of microtubules with TTC tips is equal to the shrinking velocity of microtubules with pure T-tubulin tips and when these two velocities are different from each other.

3.4 Behavior of total T-tubulin concentration in the steady state when there is a unique shrinking velocity for microtubules ($p_m = p_d$)

Equations 29 and 30 below are written in the sum form using Equations (21-24).

$$p_d\alpha[P_- - P_-(1)] + p_m\gamma[\Pi_- - \Pi_-(1)]$$
$$+f_cP_+ - (p_d + p_m)\alpha P_- - (p_d + p_m)\gamma\Pi_- = 0, \tag{31}$$

$$p_d\beta[P_- - P_-(1)] + p_m\zeta[\Pi_- - \Pi_-(1)]$$
$$+f_c'\Pi_+ - (p_d + p_m)\beta P_- - (p_d + p_m)\zeta\Pi_- = 0, \tag{32}$$

In the case of $p_m = p_d$, $P_- + \Pi_-$ written as below:

$$P_- + \Pi_- = -[P_-(1) + \Pi_-(1)] + \frac{f_c}{p_d}P_+ + \frac{f_c'}{p_d}\Pi_+. \tag{35}$$

Note that $P_- + \Pi_-$ is independent of the bio-statistical parameters.

Although we cannot find an explicit expression of $P_-(n)$ and $\Pi_-(n)$ in this case, we have the necessary tools to check the behavior of total T-tubulin concentration in the steady state.

As a next step, P_0 and Π_0 are calculated. To find P_0 and Π_0, we use a normalization equation:

$$P_0 + \Pi_0 + \sum_{n=1}^{\infty}(P_+(n,t) + \Pi_+(n,t)) + \sum_{n=1}^{\infty}(P_-(n,t) + \Pi_-(n,t)) = 1. \tag{36}$$

The above equation can be rewritten in the steady state as:

$$P_0 + \Pi_0 + P_+ + \Pi_+ + P_- + \Pi_- = 1. \tag{37}$$

As we see, there is no need to have the explicit expression for $P_-(n)$ and $\Pi_-(n)$ in above equation; all we need is $P_- + \Pi_-$ which we already have.

By substituting the relevant expressions in equation (37), P_0 can be calculated:

$$P_0 + \theta P_0 + \frac{(1+\theta)C}{1-(A+C)}P_0 + \frac{(1+\theta)A}{1-(A+C)}P_0 - (X + Y\theta)P_0$$
$$\frac{f_c}{p_d}\left[\frac{(1+\theta)C}{1-(A+C)}\right]P_0 + \frac{f_c'}{p_d}\left[\frac{(1+\theta)A}{1-(A+C)}\right]P_0 = 1. \tag{38}$$

Therefore

$$P_0 = \frac{1}{Z(1+\theta)}, \tag{39}$$

where

$$Z = (1+\frac{f_c}{p_d})(\frac{C}{1-(A+C)}) + (1+\frac{f_c'}{p_d})(\frac{A}{1-(A+C)}) - X. \tag{40}$$

To determine the behavior of total T-tubulin concentration, time evolution equations for the free subunits are necessary. These complimentary equations can be written with the help of Figure 3.3 and 3.4 as:

$$\frac{\mathrm{d}C_T^*}{\mathrm{d}t} = -p_g \left[\sum_{n=1}^{\infty} (P_+(n,t) + \Pi_+(n,t))\right] + \alpha' C_d^*, \tag{41}$$

$$\frac{\mathrm{d}C_T^{**}}{\mathrm{d}t} = -p_c \left[\sum_{n=1}^{\infty} (P_+(n,t) + \Pi_+(n,t))\right] + \alpha' C_d^{**}, \tag{42}$$

$$\frac{\mathrm{d}C_d^{**}}{\mathrm{d}t} = p_d \sum_{n=1}^{\infty} P_-(n,t) - \alpha' C_d^{**}. \tag{43}$$

and

$$\frac{\mathrm{d}C_d^{*}}{\mathrm{d}t} = p_m \sum_{n=1}^{\infty} \Pi_-(n,t) - \alpha' C_d^{*}. \tag{44}$$

In the above equations, C_T^* is the T-tubulin concentration without drug bonding, C_T^{**} is the concentration of T-tubulin with drug bonding, C_d^{**} and C_d^* are D-tubulin concentrations released from the polymerization cycle of microtubules with TTC and with TT tips respectively, and α' is the regeneration rate.

We also have the conservation of tubulin subunits expressed below, with C_0 the overall concentration of tubulin subunits as:

$$C_T^* + C_T^{**} + C_d^* + C_d^{**} + \sum_{n=1}^{\infty} nP_+(n,t) + \sum_{n=1}^{\infty} n\Pi_+(n,t) = C_0, \tag{45}$$

when

$$C_T^* + C_T^{**} = C_T. \tag{46}$$

and

$$C_d^* + C_d^{**} = C_d. \tag{47}$$

By eliminating C_d from the above equations, the kinetic equations for total free T-tubulin concentration can be expressed as:

$$\frac{\mathrm{d}C_T}{\mathrm{d}t} = -(p_g + p_c)\left[\sum_{n=1}^{\infty}(P_+(n,t) + \Pi_+(n,t))\right]$$
$$-\alpha'\left[\sum_{n=1}^{\infty} n(P_+(n,t) + \Pi_+(n,t))\right] + \alpha'(C_0 - C_T). \tag{48}$$

The interesting thing about this equation is that by eliminating the C_d, we do not need explicit expressions for $P_-(n,t)$ and $\Pi_-(n,t)$.

The left hand side of the above equation is zero in the steady state. The self-consistent equation for the population of total T-tubulin concentration is:

$$C_0 - C_T^0 = (p_g + p_c)\frac{1}{Z\alpha'}(\frac{A+C}{1-(A+C)}) + \frac{1}{Z}(\frac{A+C}{(1-(A+C))^2}). \tag{49}$$

Behavior of total free T-tubulin concentration can be calculated by numerical methods. If $p_m = p_d$, the self consistent equation is independent of bio-statistic parameters and bio-ratio parameters.

The behavior of total free T-tubulin concentration as a function of regeneration rate is considered for in the following cases:

- In figure 3.5 this behavior is determined,i n the absence of drugs, when $p_g = 0.1$, $p_d = 1$, and $f_c = f \exp \frac{C_T}{C_f}$, with $f = 0.06$ and $C_f = 3$ and $\gamma = 1$.
- In figure 3.6 this behavior is determined in the presence of colchicine when we have all of the above sets of parameters plus $p_d = p_m = 1$, $f_c' = 0.5 f_c$ and $p_c = 0.05$.
- In figure 3.7 this behavior is determined when $p_c = 0.06$, $f_c' = 0.6 f_c$, $f_c' = f_c$, $f_c' = 2f_c$, $f_c' = 3f_c$.

We will discuss the our numerical results in the last section of this chapter.

3.4.1 When shrinking rate for microtubules with T-Tubulin-colchicine tips is less than shrinking rate for microtubules with T-Tubulin-colchicine ($p_m < p_d$)

When the shrinking rate for microtubules with TTC tips is less than the shrinking rate for microtubules with TTC, the sum of the probabilities of shrinking microtubules with TTC tips, (Π_-) and TT tips (P_-) are:

$$P_- = -\frac{p_d}{p_m}P_-(1) - \frac{f_c\zeta}{p_m(\gamma\beta - \alpha\zeta)}P_+ + \frac{f_c'\gamma}{p_m(\gamma\beta - \alpha\zeta)}\Pi_+, \tag{50}$$

and

$$\Pi_- = -\frac{p_m}{p_d}\Pi_-(1) + \frac{f_c\beta}{p_d(\gamma\beta - \alpha\zeta)}P_+ - \frac{f_c'\alpha}{p_d(\gamma\beta - \alpha\zeta)}\Pi_+. \tag{51}$$

With the help of Equation (37), we can find P_0, which is:

$$P_0 = \frac{1}{Z'}$$

when

$$Z' = \left[\frac{f_c'}{(\gamma\beta - \alpha\zeta)}(\frac{\alpha}{p_d} + \frac{\gamma}{p_m}) + 1\right]\frac{(1+\theta)A}{1-(A+C)} - (\frac{p_g + p_c}{p_d} + 1)\theta$$
$$+ \left[\frac{f_c}{(\gamma\beta - \alpha\zeta)}(\frac{\zeta}{p_m} + \frac{\beta}{p_d}) + 1\right]\frac{(1+\theta)A}{1-(A+C)} + (\frac{p_g + p_c}{p_m} + 1).$$

Again, we can determine the behavior of total T-tubulin concentration. The results are dependent on bio-statistical parameters.

We do not intend to go through the statistical calculations here, but only conclude that to obtain more information on the behavior of polymer mass in the steady state, It is essential to have more information about the statistics of shrinking microtubules.

3.5 Conclusions

The mathematical model built in this chapter assumes drug tips (TTC) cannot block the frequency of catastrophe. Microtubules with drug tips can

shrink, although they shrink more slowly than pure tubulin tips. This behavior has been seen in microtubules which interact with high concentrations of antimitotic drugs, including colchicine [48].

In the process of extending the model, bio-statistical parameters were introduced. The calculations show that: if the shrinking velocities for microtubules are the same, the behavior of the free total T-tubulin concentration will be independent of bio-statistical parameters. We can summarize the behavior of total T-tubulin concentration as follows:

- The maximum free T-tubulin concentration in the steady state is related to the state in which there is no colchicine in the solution, Fig. 3.5.

- Figs. 3.5 and 3.6 present the total free T-tubulin concentration in the steady state and in the presence of high concentrations of colchicine. It is assumed that shrinking velocities for microtubules with and without drug tips are the same. The assembly rate with the addition of T-tubulin p_g is assumed to be 0.1, and the assembly rate with the addition of T-tubulin-colchicine (p_c) is considered to be 0.05 in Fig. 3.5 and 0.06 in Fig. 3.6.

- The total T-tubulin concentration shows a slight increase when p_c and the frequency of catastrophe increase at the same time, Fig. 3.7.

Vandecandelaere et al. showed [48] that total T-tubulin increases slightly in vitro in the presence of high concentrations of T-tubulin-colchicine complex in the steady state. They explain that the reason is due to the fact that tubulin-GDP-containing microtubules are only stabilized by addition of pure T-tubulin. Adding T-tubulin-colchicine complex does not guarantee such a stabilization and therefore the number of catastrophe events experienced by microtubules increases and total free T-tubulin concentration shows a small increase as well.

By increasing the amount of p_c to 0.06 in Figure 3.6, we can see the expected drop in the amount of tubulin concentration. When catastrophe frequency increases at the same time, the total T-tubulin concentration shows a small increase, which agrees Vandecandelaere's experimental results.

One might initially consider the assumption that the shrinking velocities are the same for microtubules with and without drug tips as a weakness of this model. Upon closer analysis, even in the presence of pure T-tubulin, the

shrinking velocity displays independent behavior; it is not a function of free sub-units. Therefore, as a good approximation, the shrinking velocity can be considered as a constant parameter. In conclusion, these assumptions lead to the results which are similar with those reported in biological experiments.

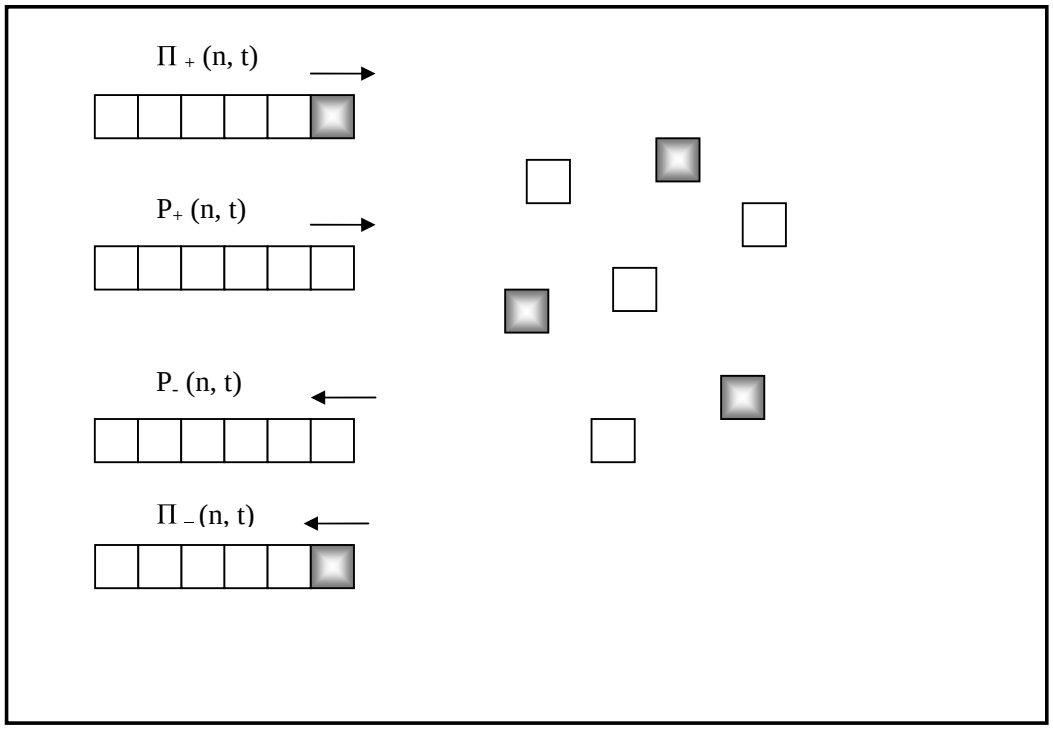

Figure 3.1: Boxes with shadow indicate T-tubulin-colchicine subunits and colorless boxes are T-tubulin subunits in this view. Two groups of polymerized microtubules, with TTC tips and with TT tips are also shown.

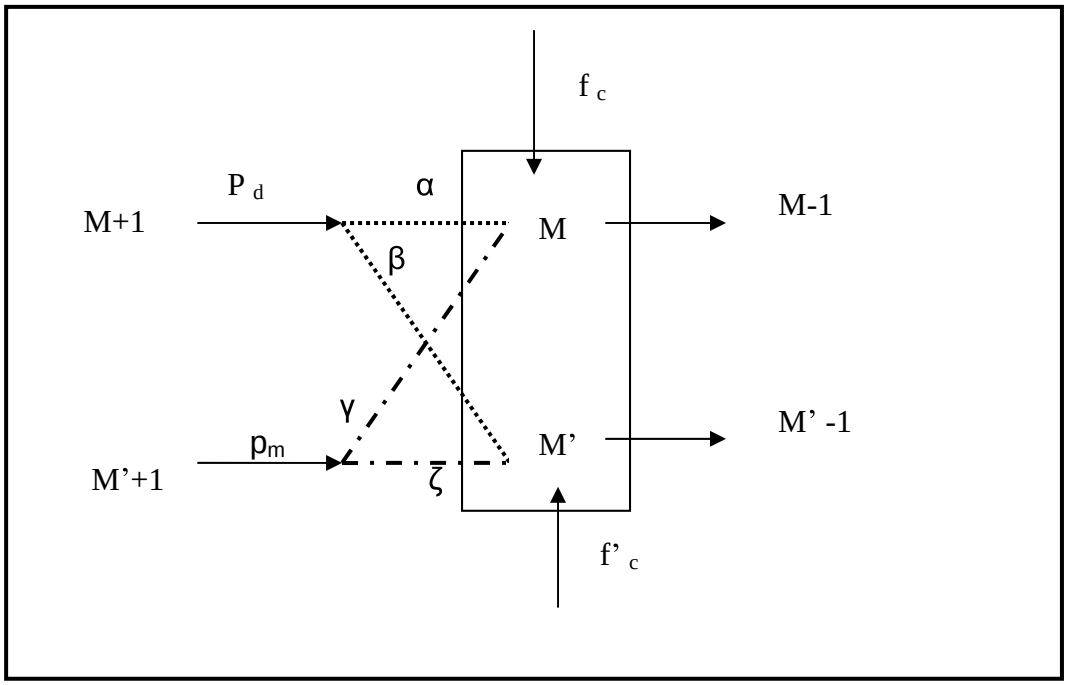

Figure 3.2: With the probability of α, a microtubule with TT tip and length M+1 can be reduced to a microtubule with the length M with the same tip and with the probability of β can be reduced to a microtubule with the length M and TTC tip. Same thing can happen when reducing a microtubule with the length M+1 and TTC tip.

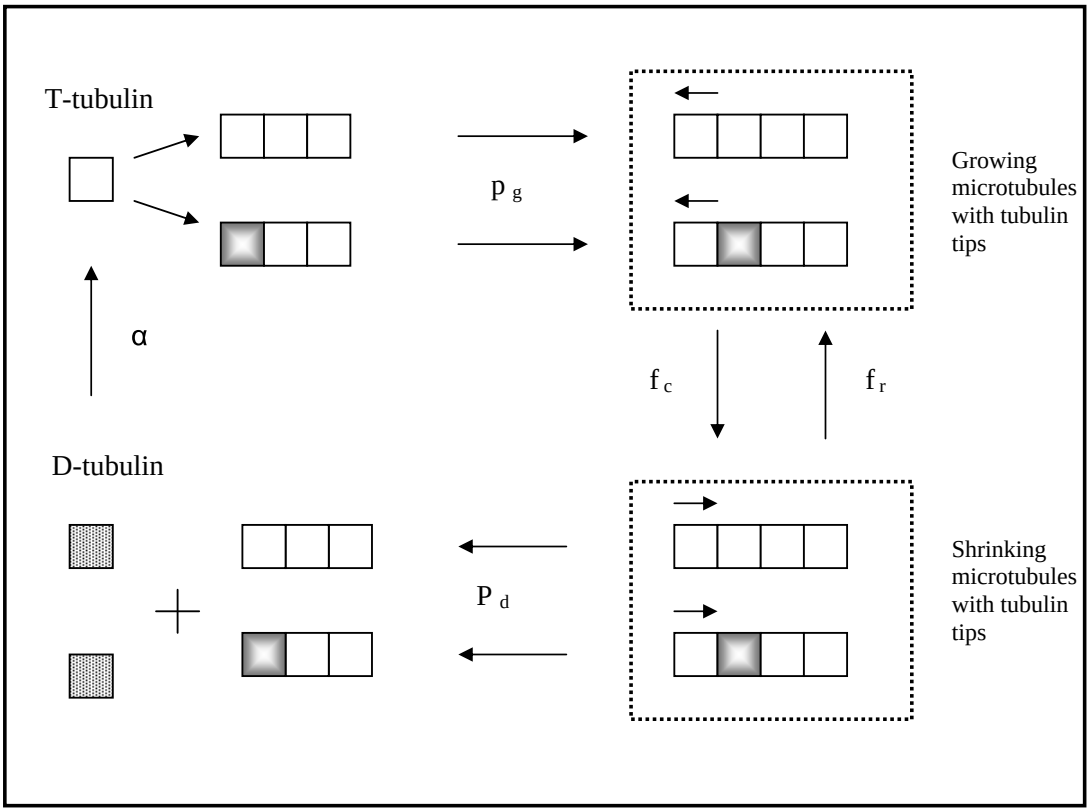

Figure 3.3: Microtubules with TT tips are reduced in size with the frequency of catastrophe f_c or rescued by the frequency f_r (the rescue frequency is neglected in the mathematical model). The shrinking velocity is p_d. During the shrinking stage D-tubulin is released into the solution. Regeneration occurs in this system at rate α.

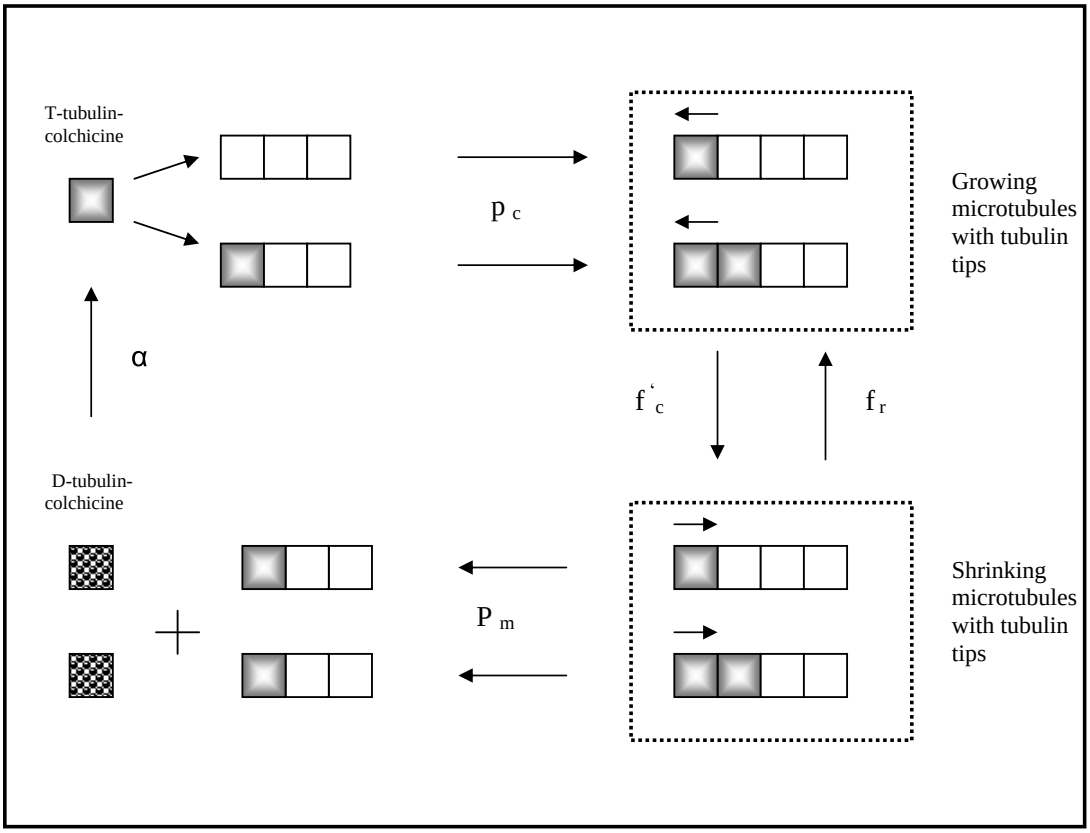

Figure 3.4: Microtubules with TTC tips are reduced in size with the frequency of catastrophe f_c' or rescued by the frequency f_r'(the rescue frequencies is neglected in the mathematical model). The shrinking velocity is p_m. During the shrinking stage D-tubulin-colchicine is released into the solution. Regeneration occurs in this system at rate α.

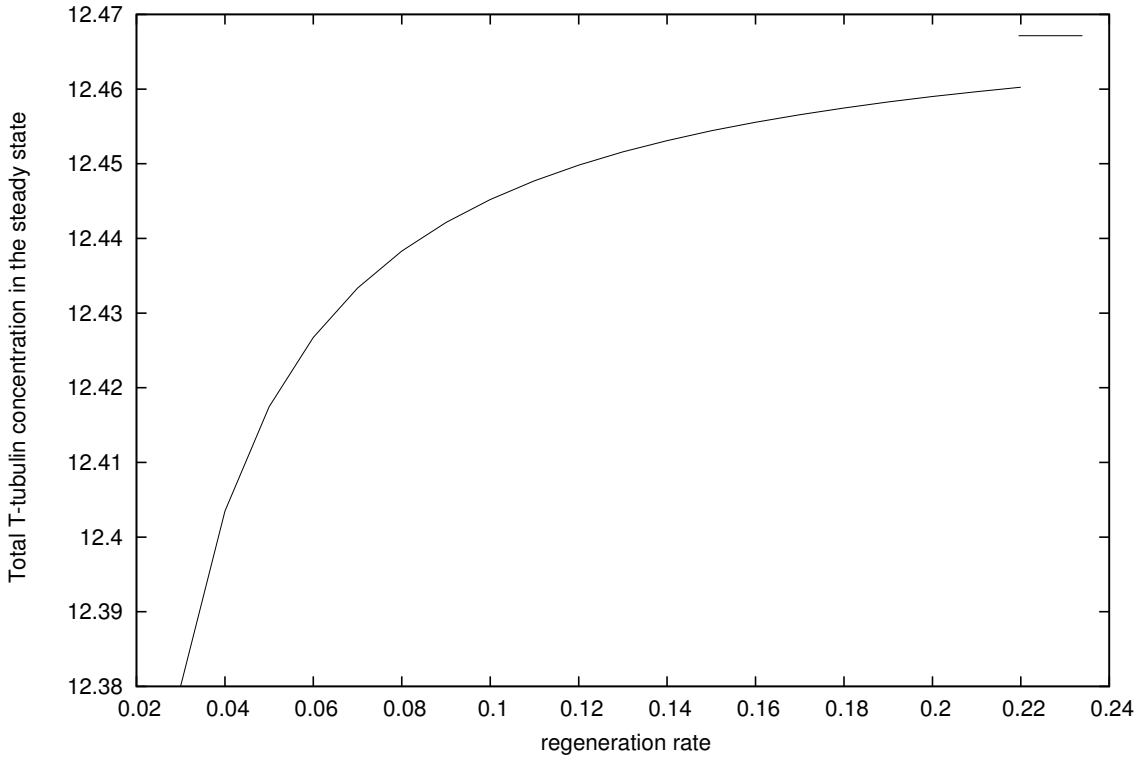

Figure 3.5: This figure indicates the concentration of free total T-tubulin in the absence of colchicine. The parameters are: $C_0 = 120$, $p_g = 0.1$, $p_d = 1$, $p_c = 0$, $f = 0.06$, $C_f = 3$, $\gamma = 1$.

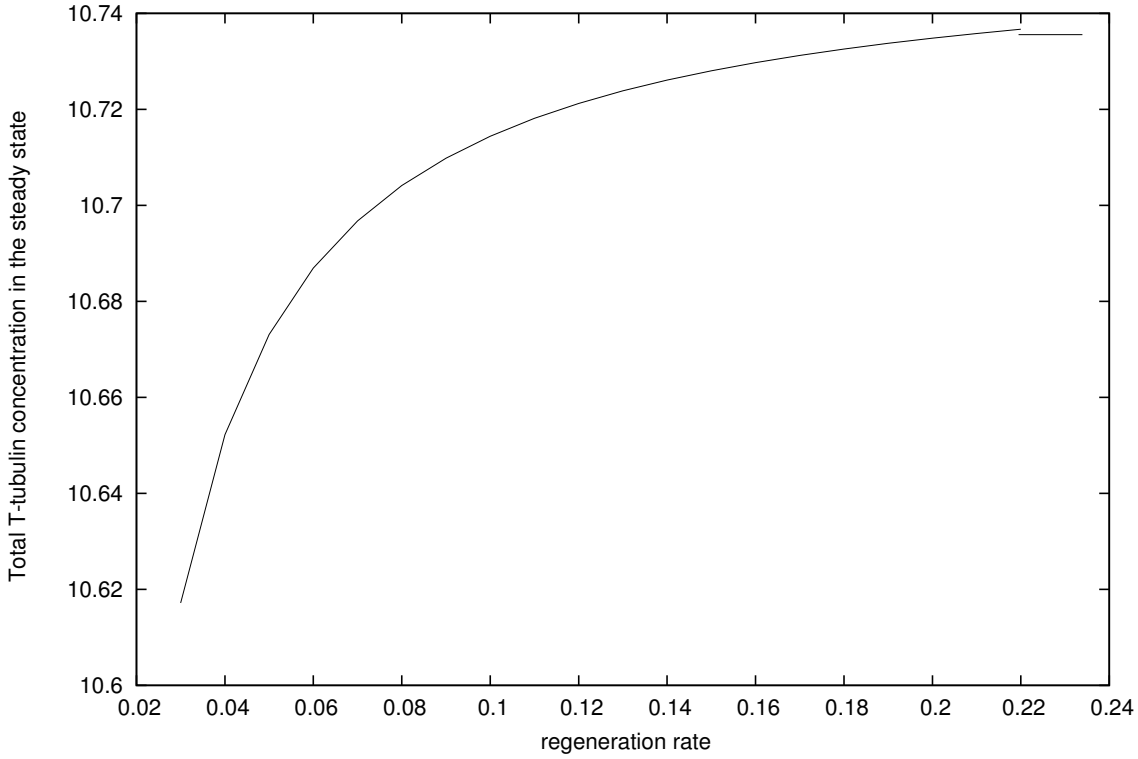

Figure 3.6: In this figure the behavior of free total T-tubulin concentration in the presence of colchicine when microtubules with TTC tips experience catastrophe. $p_d = 1$, $p_m = 1$ and $p_c = 0.05$.

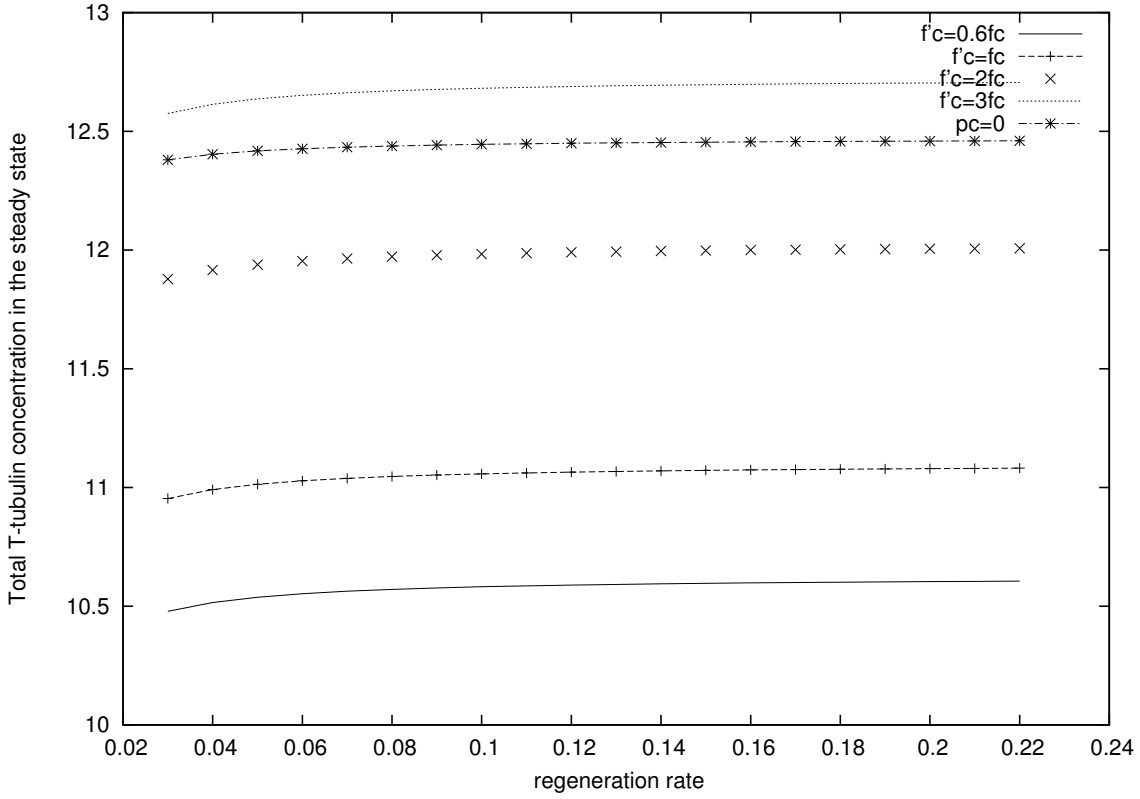

Figure 3.7: This figure indicates the concentration of free total T-tubulin in the presence of colchicine when $p_d = p_m = 1$ and $p_c = 0.06$ and $f_c' = 0.6f_c$, $f_c' = f_c$, $f_c' = 2f_c$, $f_c' = 3f_c$.

Chapter 4

Treadmilling Behavior in the Dynamics of Microtubules

4.1 Introduction

Previous chapters discussed mathematical models of co-polymerization of microtubules. The main focus was on plus ends of microtubules in vitro. With in vitro experiments, using the seed method, a microtubule can grow from both ends. In vivo, minus ends of microtubules are thought to be capped by the centrosome, whereas plus ends are free and display dynamic instability.

Recent improvements in the sensitivity of cameras for fluorescence imaging and the introduction of methods to reduce flurophore-induced photodamage in living cells [49] have allowed for a more detailed view of larger areas of the microtubule cytoskeleton over longer times. This has led to several interesting new observations of microtubule dynamics in interphase cells, including the recent discovery by Rodionov and Borisy [50] of treadmilling behavior of individual microtubules during interphase. These researchers examined melanophore cell fragments micro-injected with x-rhodamine-tubulin to determine how microtubules are organized in the cytoplasm in the absence of a centrosome. In the cell fragments, microtubules were seen to organize themselves into a radial array, which frequently released microtubules from its center. Released microtubules can experience dynamic instability from both ends.

Individual microtubules can experience growing from one end and shrink-

ing from another end in such a way that the tubulin concentration stays constant over time. This behavior, known as treadmilling, can be seen in an individual microtubule in vivo with two free ends for a short period of time in a less specifically regulated way, simply by the random chance that normal dynamic instability becomes coordinated between the two microtubule ends, resulting in net growth at one end and net shortening at the other. There are two recent examples of this. Keating et al. [51] examined microtubule dynamics at the centrosome in PtK cells and found that the minus end of a microtubule released from the centrosome could shorten rapidly, with intermittent pauses, toward its randomly growing and shortening plus end. If plus-end dynamic instability resulted in net growth, the microtubule could be ejected from the centrosome region by treadmilling, until it was eventually consumed by shrinking at the minus end.

In addition to these examples of individual microtubule behavior, there are also recent examples of coordinated net assembly/disassembly at the two ends of microtubules in a large ensemble of microtubules.

Pure tubulin treadmilling in a minus-to-plus direction was reported by Walker et al. [28] in 1988. Several years later Hotani and Horio [27] used dark field microscopy and observed treadmilling of individual MAP-containing microtubules at rates similar to those for pure tubulin, but in a plus-to-minus direction. This observation built up the idea that the binding of MAP's could suppress the phase transition of dynamic instability and bias the kinetic properties of the two ends to allow for treadmilling [27].

Treadmilling steady state is the second type of steady state that has been seen in the dynamics of microtubules. Recently [52] the novel steady state of microtubules was observed in vivo. This steady state was observed in the presence of persistent growth of individual microtubules. In fact, the amount of polymer does not change over time and steady state occurs in this case in the presence of the cell boundary. Fluctuation of growth and shortening near the cell margin, on the average, equate to each other because persistent growth up to the cell boundary restores polymer lost by shortening from the boundary. Thus cellular levels of microtubule polymer remain constant even in the presence of persistent growth of individual MTs.

The steady state of a microtubule assembly has received much attention recently from a mathematical point of view. In the mathematical model presented by Dogterom and Leibler, microtubules are assembled to nucleate and grow from plus ends in the absence of any boundary. When the multiplication of catastrophe frequency and shrinking rate are greater than multiplication

of rescue frequency and growth rate, the model has a stationary solution in the form of an exponentially decaying distribution of lengths [11]. This model is studied in more detail in the next section. The recent observation of a steady state solution of microtubule dynamics in the presence of a cell boundary and persistently growing microtubules has been mathematically modeled by Govindan and Spillman [48].

The main object of this chapter is to provide a descriptive mathematical model to express the treadmilling steady state in an ensemble of microtubules.

This chapter is organized as follows:

- The continuous model for the nucleation and polymerization of microtubules (Dogterom's model) and steady state solutions is reviewed.
- The extension of Dogterom's model for growing microtubules from both ends and steady state solutions under the treadmilling condition are discussed in Section 4.3.
- The behavior of T-tubulin concentration in the steady state will be investigated in the regeneration system and the stability condition is considered at the end of the chapter.

4.2 Dogterom model

By neglecting concentration variation in the process of assembly and disassembly of microtubules, dynamic equations in the continues form can be written as:

$$\partial_t P_+(l,t) = -f_c P_+(l,t) + f_r P_-(l,t) - v_g \partial_l P_+(l,t) \qquad (1a),$$

and

$$\partial_t P_-(l,t) = +f_c P_+(l,t) - f_r P_-(l,t) - v_s \partial_l P_-(l,t) \qquad (1b).$$

where $P_+(l,t)$ and $P_-(l,t)$ are the probabilities of length distribution of microtubules in the growing or shrinking state. Also, f_c and f_r are the frequencies of catastrophe and rescue and v_g and v_s are the growing and shrinking velocities.

These equations can be solved analytically with appropriate boundary conditions. The nucleation rate ν itself defines a boundary condition for the length distribution of growing microtubules, $P_g(l,t)$ at $l = 0$.

The nucleation process has been investigated in greater detail in references [19] and [53]. The nucleation rate ν depends on the initial concentration C_0 of tubulin dimers, but it is rather independent of temporal variation of C_T, as observed in recent experiments [53], [19]. Accordingly, for a given initial concentration C_0, it is assumed that nucleation rate ν is constant. Based on that, the boundary condition is:

$$P_g(l=0,t) = \frac{\nu}{v_g}. \tag{2}$$

The boundary condition for shrinking microtubules is:

$$P_s(l=\infty,t) = 0. \tag{3}$$

Because the transition from growing to shrinking is the only source for shrinking microtubules, $P_g(l=\infty,t)$ vanishes for large values of l.

As discussed in the first chapter, the microtubule length distribution can be placed in one of two categories: the unbound or bound state. In the unbound state, the probability distribution is not a steady state distribution; the microtubule length distribution should be strongly asymmetric early after the beginning of growth and then tend with time toward a Gaussian distribution. It is of the form:

$$\begin{aligned} P(l,t) &= P_+(l,t) + P_-(l,t) \\ &= \frac{1}{(2\Pi Dt)^{1/2}} \exp\left[\frac{-(l-Jt)^2}{2Dt}\right] \\ &\left[1 + C\left(\frac{(C-Jt)^3}{D^3t^2} - \frac{3(l-Jt)}{D^2t}\right) + ...\right], \end{aligned} \tag{4a}$$

when

$$D = \frac{2f_cf_r(v_g+v_s)^2}{(f_c+f_r)^3}, \tag{4b}$$

and

$$J = \frac{v_gf_r - v_sf_c}{f_c+f_r}. \tag{4c}$$

C is a correction coefficient.

In the steady state, the left hand side of the kinetic equations vanishes and the steady state solution will be:

$$P^0_{g,s}(l) = \frac{\nu}{v_{(g,s)}} \exp A.l, \tag{5}$$

where $A = \frac{f^0_r}{v_s} - \frac{f^0_c}{v_g}$.

This solution can be interpreted as a steady state solution in the presence of plus ends of a microtubule only if the second term in A is greater than the first term.

In this case the integrated length of all microtubules per unit volume is:

$$L(t) = \int_0^\infty dl[P_g(l,t) + P_s(l,t)].l. \tag{6}$$

$L(t)$ is independent of the length in the steady state. Polymer mass also stays constant.

4.3 Mathematical model for the presence of two ends

In this work the regenerating system is considered as a basis for microtubules which grow from both ends. In Fig 4.1, a schematic view of the model is shown. The regeneration factor α is global and unique for both ends, while there is a separate cycle of polymerization for each end.

If we consider the two different phases of MTs and neglect concentration variations, the following detailed balanced equations can be written for the dynamics of microtubules [11]:

$$\partial_t P_{g_{(i)}} = -f_{c_{(i)}} P_{g_{(i)}} + f_{r_{(i)}} P_{s_{(i)}} - v_{g_{(i)}} \partial_l P_{g_{(i)}}, \tag{7a}$$

and

$$\partial_t P_{s_{(i)}} = +f_{c_{(i)}} P_{g_{(i)}} - f_{r_{(i)}} P_{s_{(i)}} + v_{s_{(i)}} \partial_l P_{s_{(i)}}, \tag{7b}$$

where i stands for the (+) or (-) end of a microtubule and f_c is the frequency of catastrophe and f_r is frequency of rescue; v_g and v_s are the velocities of growing and shrinking respectively.

It is assumed that the plus and minus ends of MT's experience independent stochastic processes, so by choosing appropriate dynamic parameters $(v_{s_i}, v_{g_i}, f_{c_i}, f_{r_i})$ and with the help of Eq. (7), the dynamic instability behavior of each end can be described mathematically. The above equations have to be supplemented by boundary conditions. In this work, we assumed

a spontaneous nucleation with the rate ν instead of nucleation on a stable centrosome.

Immediately after nucleation, some of the total T-tubulin in solution interacts with the polymerization cycle of the plus end and some with the minus end. The time variation of T-tubulin concentration in each cycle can be written using the following equations [53]:

$$\partial_t C_{T_{(i)}} = -\gamma v_{g_{(i)}} \int_0^{a(b)} P_{g_{(i)}}(l,t)\mathrm{d}l + \alpha C_{d_{(i)}}, \tag{8a}$$

and

$$\partial_t C_{d_{(i)}} = +\gamma v_{s_{(i)}} \int_0^{a(b)} P_{s_{(i)}}(l,t)\mathrm{d}l - \alpha C_{d_{(i)}}. \tag{8b}$$

where i indicates the polymerization cycle of the plus end or minus end and γ is a length factor describing the number of tubulin dimers that are incorporated in a unit length of microtubules. The length distribution or age of the plus ends has been considered between 0 and a and for the minus ends, between 0 and b.

We also emphasize that:

$$C_{T_{(+)}} + C_{T_{(-)}} = C_T. \tag{9}$$

The conservation of tubulin dimers can be expressed by the following conditions:

$$C_{T_{(+)}} + C_{d_{(+)}} + \gamma L_{(+)} = mC_0, \tag{10a}$$

$$C_{T_{(-)}} + C_{d_{(-)}} + \gamma L_{(-)} = nC_0, \tag{10b}$$

and

$$m + n = 1, \tag{10c}$$

where C_0 is the overall concentration of tubulin dimers. $L_{(i)}(t)$ is the integrated length of all microtubules per unit volume for each end and is equal to:

$$L_{(i)}(t) = \int_0^{a(b)} l \left[P_{g_{(i)}}(l,t) + P_{s_{(i)}}(l,t)\right] \mathrm{d}l, \tag{11a}$$

and

$$L(t) = L_{(+)} + L_{(-)}. \tag{11b}$$

Where L(t) is the total average of length. With the help of Eqs. (8-10), the time variation of the T-tubulin concentration can be expressed by the following equation:

$$\partial_t C_T = -\gamma \int_0^a \left[v_{g_{(+)}} P_{g_{(+)}} + \alpha l (P_{g_{(+)}} + P_{s_{(+)}}) \right] \mathrm{d}l$$
$$-\gamma \int_0^b \left[v_{g_{(-)}} P_{g_{(-)}} + \alpha l (P_{g_{(-)}} + P_{s_{(-)}}) \right] \mathrm{d}l + \alpha (C_0 - C_T). \tag{12}$$

4.4 Stationary stage

By definition, the steady state for microtubule dynamics implies time-invariant kinetic parameters. The steady state solution for Eq. (7) is then:

$$P^0_{g,s_{(i)}}(l) = \frac{\nu}{v_{(g,s)_{(i)}}} \exp A.l_{(i)}. \tag{13}$$

where $A = \frac{f^0_{r_{(i)}}}{v_{s_{(i)}}} - \frac{f^0_{c_{(i)}}}{v_{g_{(i)}}}$. We have assumed that in the treadmilling steady state, the length distribution of the plus end is between (0 to ∞) and the distribution for the minus end is (0 to b). The consumed T-tubulin on the minus end should be equal to the tubulin released by the plus end. This yields:

$$\gamma v_{g_{(-)}} \int_0^b P^0_{g_{(-)}}(l) \mathrm{d}l = \gamma v_{s_{(+)}} \int_0^\infty P^0_{s_{(+)}}(l) \mathrm{d}l. \tag{14}$$

This assumption yields a condition for the length distribution of the minus end, i.e.:

$$b = \frac{1}{A} \ln \left(1 + A \frac{v_{g_{(+)}}}{f_{c_{(+)}}} \right). \tag{15}$$

In this calculation it is assumed that the frequency of rescue in the steady state is negligible for the plus end. For the minus end, the frequency of catastrophe is much smaller than the frequency of rescue. In the following, the behavior of T-tubulin concentration is studied in the treadmilling steady state and in the presence of dynamic instability for each end.

4.4.1 Behavior of T-tubulin concentration in the treadmilling steady state

In the stationary phase the left hand side of Eq. (12) vanishes. It is assumed that the frequency of catastrophe and rescue both exhibit exponential C_T dependence [53]. With the help of Eq. (15), the stationary T-tubulin concentration C_T^0 can be determined by a nonlinear self-consistent equation:

$$C_0 - C_T^0 = \frac{\gamma\nu v_{g_{(+)}}}{f_{c_{(+)}}}\left(\frac{1}{\alpha} + \frac{1}{f_{c_{(+)}}}(1 + \frac{v_{g_{(+)}}}{v_{s_{(+)}}})\right) + \frac{\gamma\nu}{A\alpha}\left[\exp(Ab) - 1\right] + \frac{\gamma\nu}{A^2}(\frac{1}{v_{g_{(-)}}} + \frac{1}{v_{s_{(-)}}})\left[1 + \exp(Ab)(-1 + Ab)\right]. \quad (16)$$

where $A = \frac{f^0_{r_{(-)}}}{v_{s_{(-)}}} - \frac{f^0_{c_{(-)}}}{v_{g_{(-)}}}$.

$$f_c = f\exp(\frac{-C_T}{C_f}), \quad (17)$$

and

$$f_r = f'\exp(\frac{+C_T}{C_{f'}}), \quad (18)$$

while f and f', C_f and $C_{f'}$ are constant. The behavior of T-tubulin concentration has been investigated via numerical analysis as shown below.

In Fig 4.2, the T-tubulin concentration in the treadmilling steady state is shown as a function of regeneration factor.

4.4.2 Numerical results

This section, presents a mathematical model for the dynamics of a microtubule when it grows from both ends. It is assumed that each end could experience dynamic instability. The ensemble of the microtubules can reach the treadmilling steady state for a short time in this case. The behavior of T-tubulin concentration in the steady state as a function of regeneration rate was analyzed through numerical calculations.

As anticipated, It can be seen in Fig 4.2.:

- The amount of T-tubulin concentration is a function of the regeneration factor for small α and independent of regeneration factor when α is large enough.
- The amount of T-tubulin concentration in the steady state decreases in the presence of a minus end.
- The nucleation rate is another factor which is involved in the amount of T-tubulin concentration the polymer mass is directly proportional to this factor.

  In general, the presence of minus ends directly affects the polymer mass and the T-tubulin concentration in the steady state in the way that presence of minus ends increases polymer mass.

4.5 Stability condition

The system in the steady state can be perturbed by adding a small amount of T-tubulin, C_T^1 to the concentration of T-tubulin in the steady state, C_T^0 . C_T^1 can affect the polymerization cycle of the plus end or the minus end. In this paper, it is assumed that injected T-tubulin affects the cycle of the minus end:

$$P_{g,s} = P^0_{g,s_{(+)}} + P^0_{g,s_{(-)}} + P^1_{g,s_{(-)}}. \tag{19}$$

and

$$C_T = C_T^0 + C_T^1. \tag{20}$$

These two expressions should be substituted in the kinetic equations for the probability of growing and shrinking, and also in the expressions we have for frequency of catastrophe and frequency of rescue. The transition frequencies are given by:

$$f_c = f \exp -\frac{C_T}{C_f} = f \exp -\frac{C_T^0 + C_T^1}{C_f} = f \exp -\frac{C_T^0}{C_f} \exp -\frac{C_T^1}{C_f}. \tag{21}$$

C_T^1 tends to zero, so the second term can be estimated as one. Therefore as a good approximation, the frequency of catastrophe after perturbation is equal to the frequency of catastrophe in the steady state.

The frequency of rescue is given by:

$$f_r = f \exp \frac{C_T}{C'_f} = f \exp \frac{C^0_T + C^1_T}{C'_f} = f \exp \frac{C^0_T}{C'_f} \exp \frac{C^1_T}{C'_f}. \tag{22}$$

This expression can be rewritten as:

$$f^1_r = +f^0_r \frac{C^1_T}{C'_f}. \tag{23}$$

Here f^1_r is the first order contribution of an expansion of the rescue rate $f_r = f^0_r + f^1_r + ...$ with respect to the perturbation C^1_T.

C_f, C'_f and f are all constant in above equations. The model focuses on the minus ends of microtubules. Minus ends are more stable and in general experience a small amount of catastrophe. By perturbing the system and adding a small amount of C_T to the system, the frequency of catastrophe drops even more due to the exponential decay behavior of the catastrophe frequency. Therefore, the term $f^1_c p^0_g$ is negligible, and since f^0_c is very small, the effect of it on the small perturbed growing distribution p^1_g is negligible. The perturbed concentration of growing and shrinking obeys the following dynamics:

$$\partial_t P^1_{g_{(-)}} = +f^0_r P^1_{s_{(-)}} + f^1_r P^0_{s_{(-)}} - v_{g_{(-)}} \partial_l P^1_{g_{(-)}}, \tag{24a}$$

and

$$\partial_t P^1_{s_{(-)}} = -f^0_r P^1_{s_{(-)}} - f^1_r P^0_{s_{(-)}} + v_{s_{(-)}} \partial_l P^1_{s_{(-)}}. \tag{24b}$$

Eq. (24) have constant coefficients, so their solution depends exponentially on time .

C^1_T may be written as:

$$C^1_T = A \exp(\sigma t) + C.C, \tag{25}$$

where $C.C$ denotes the complex conjugate and A is a constant.

The above equations have the analytical form of:

$$P^1_s(l,t) = \frac{\nu f^0_r}{-v_s c_f \sigma} \exp\left(\sigma t + \frac{f^0_r l}{v_s}\right) \left[\exp(\frac{\sigma l}{v_s}) + 1\right] A + C.C. \tag{26a}$$

and

$$P_g^1(l,t) = \frac{\nu f_r^0}{v_g c_f \sigma} \exp\left(\sigma t + \frac{f_r^0 l}{v_s}\right)$$
$$\left[k_1 \exp(\frac{\sigma l}{v_s}) + k_2 + K \exp(\frac{-\sigma l}{v_g})\right] A + C.C. \quad (26b)$$

Applying the boundary condition $p_g^1(t, l = 0) = 0$ to the Eq. (24b) yields:

$$k_1 + k_2 + K = 0. \quad (27)$$

By substituting Eq. (26a) and (26b) into Eqs. (24a) and (24b), the coefficients can be calculated as:

$$k_1 = \frac{-f_r^0}{f_r^0 + \sigma(1 + 1/\beta)}, \quad (28a)$$

$$k_2 = \frac{\sigma - f_r^0}{\sigma/\beta + f_r^0}, \quad (28b)$$

and

$$K = -(k_1 + k_2). \quad (28c)$$

Knowing the expression for perturbed distributions of growing and shrinking microtubules determines, the behavior of T-tubulin concentration.

4.5.1 The dynamics of perturbed T-tubulin concentration

Using Eqs. (12a,b), the dynamics of perturbed T-tubulin concentration C_T^1 can be expressed as:

$$\partial_t C_t^1 = -\gamma \int_0^b \left[v_{g_{(-)}} P^1_{g_{(-)}}(l,t) + \alpha l (P^1_{g_{(-)}}(l,t) + P^1_{s_{(-)}}(l,t))\right] \mathrm{d}l - \alpha C_t^1. \quad (29)$$

By substituting Eqs. (26a,b) into Eq. (29), the nonlinear dispersion relation for σ is found to be:

$$\sigma^5 v_g^2 + \sigma^4 \left[-3 v_g^2 f_r^0 \beta - v_g^2 \alpha - G l^2 f_r^0 v_g \beta\right]$$
$$+\sigma^3 \left[-2 v_g^2 (f_r^0)^2 \beta - 4 v_g^2 \alpha f_r^0 \beta + G (f_r^0)^2 l^2 v_g \beta\right]$$

$$+\sigma^2\left[-v_g^2(f_r^0)^3\beta^2 - v_g^2\alpha(f_r^0)^2(2\beta+\beta^2) + 2G(f_r^0)^3l^2\beta^3v_g + 2G(f_r^0)^3l^2v_g\beta\right]$$
$$+\sigma\left[-v_g^2\alpha(f_r^0)^3\beta^2 - v_g\beta^3l^2(f_r^0)^4G + 2G(f_r^0)^4l^2v_g\beta^2\right] = 0, \qquad (30)$$

when $\beta = \frac{v_{g_{(-)}}}{v_{s_{(-)}}}$ and $G = \frac{\gamma\nu}{c_f}$.

Here, the exponential terms are expanded and terms greater than second order in length are ignored. Since the shrinking velocity is almost ten times greater than the growing velocity, β is less than unity. Therefore, when β and β^2 had the same coefficient, we ignored the β^2 term. $1/\beta$ terms were dropped if they had the same coefficient as the $1/\beta^2$ terms.

Starting from the model equations given in Section 4.3, the system can be perturbed with respect to the stationary state by adding a small amount of C_T. This perturbation has an exponential time dependence, $\exp\sigma t$. For the exponential factor σ, we derived a non linear equation.

When the growth rate, $Re(\sigma)$, becomes positive, the system is unstable. $Re(\sigma) = 0$ is the neutral stability condition. The neutral stability condition provides an equation for the critical value $c_0 > c_{0c}$, the stationary solutions are unstable; in this case $Im(\sigma) = \omega_c$, is the Hopf frequency.

By substituting $Im(\sigma) = \omega_c$, the above equation can be broken down into its real and the Hopf frequency as a function of regeneration rate can be calculated by the imaginary part:

$$\omega_c = \frac{f_r^{0^3}\beta^2v_g - 2v_g\alpha f_r^{0^2}\beta + 2Gf_r^{0^3}l^2\beta^3}{3v_gf_r^0\beta - v_g\alpha - Gl^2f_r^0} \qquad (31)$$

4.6 Conclusions

In this chapter, the continuous mathematical model for dynamic instability of microtubules was applied to both ends of microtubules. By considering a net loss of subunits from one end and net gain of subunits from another end (the treadmilling condition), the existence of a steady state solution was determined. The behavior of T-tubulin as a function of regeneration rate was investigated. This chapter concluded with a discussion of the stability of such a system.

$$\begin{array}{ccc} \textbf{GDP} & \textbf{Tubulin- T} -- V_g \longrightarrow & \textbf{Growing MTs} \\ \uparrow & \uparrow\alpha & f_c \Updownarrow f_r \\ \textbf{GTP} & \textbf{Tubulin- D} -- V_s \longrightarrow & \textbf{Shrinking MTs} \end{array}$$

Figure 4.1: A microtubule can be polymerized from tubulin- T. Polymerization happened by the growing velocityV_g. Catastrophic and rescue frequencies are two dynamical parameters cause transition between polymerization and depolymerization stage. In the depolymerization stage, shrinking microtubule converted to tubulin- D by the shrinking velocity V_s. The cycle becomes closed by regeneration of tubulin- D at the rate α back to tubulin- t dimers.

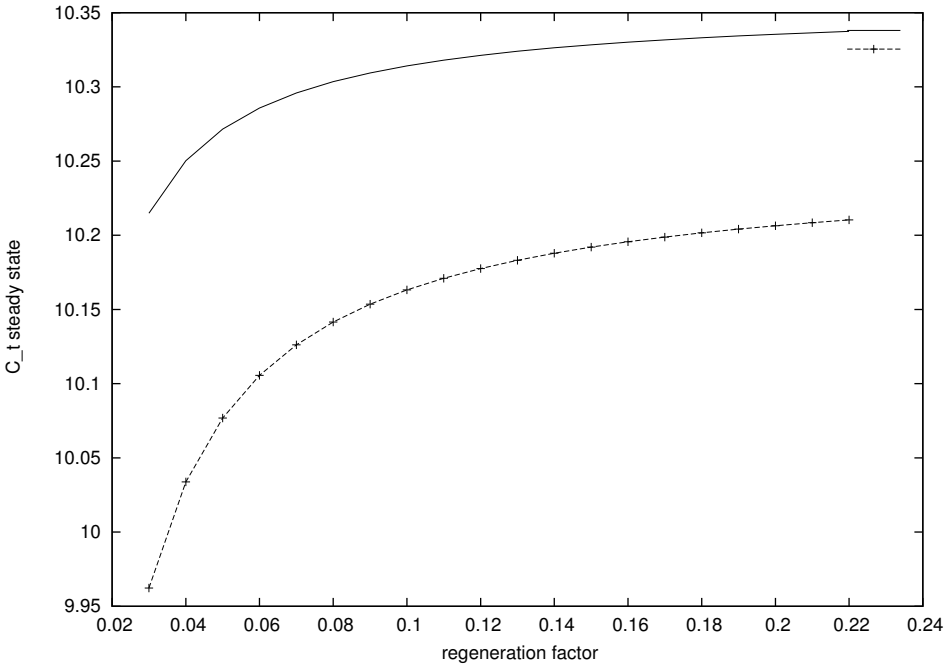

Figure 4.2: Solid line: the tubulin- T concentration for the stationary polymerization C_t^0 in the presence of the microtubule's plus ends. Point line: C_T^0 in the presence of both ends of microtubule. The parameters are $C_0 = 120$, $\gamma = 1$, $V_{g_{(+)}} = 2V_{g_{(-)}} = 0.1$, $V_{s_{(+)}} = V_{s_{(-)}} = 1$, $\beta_{(+)} = 0.1$, $\nu = 0.01$, $f = f' = 0.1$, $C_f = C_{f'} = 3$, $f_{c_{(-)}} = 0.5 f_{c_{(+)}}$.

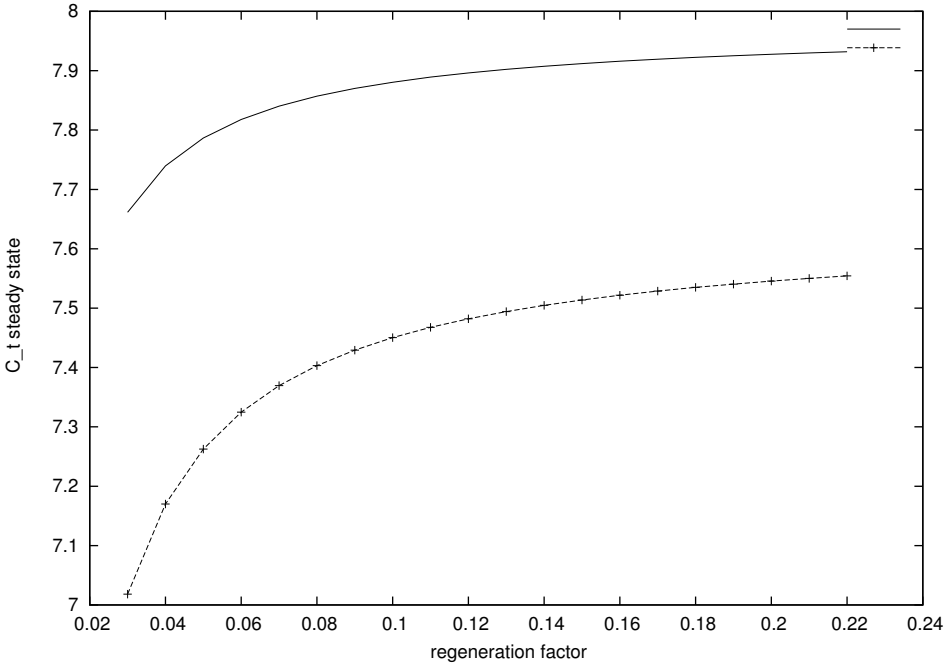

Figure 4.3: In this figure nucleation rate, $\nu = 0.05$.

Chapter 5

Summary and Outlook

The objective of this study was to develop mathematical models to describe the dynamics of microtubules. After gathering data and considering experimental results, we perused the main goal of this work: to build models to describe the copolymerization of microtubules in the presence of antimitotic agents. The fundamental steps and main results of this research follow:

- Chapter 2 extended the Hill model of polymerization of microtubules in the presence of low concentrations of colchicine. Although colchicine is still under clinical consideration for curing cancerous tumors, its irreversible bonding with tubulin subunits made it a good candidate for the first attempt at modeling. The results of analytical and numerical calculations showed an ignorable change in the steady state of polymer mass in a regeneration system. This result is in a good agreement with reported experimental results.

- Increasing the complexity of the system in chapter 3 led to a more accurate model of high concentration of colchicine. Analytical solutions for the steady state are accessible just in this specific case, but the behavior of free T-tubulin and therefore the steady state of the polymer mass can be investigated numerically. Results showed a slight increase in total free T-tubulin concentrations which can be interpret by the structure of interaction of high concentration of colchicine that adding T-tubulin-colchicine as a cap to the microtubules body does not guarantee the stability of microtubule and unlike low concentrations of colchicine, the number of catastrophe events increases and steady state

polymer mass decreases. These behavior were drawn concluded from the extended mathematical model presented.

- In the last phase, the treadmilling steady state of microtubules was studied. In this case, both ends of a microtubule experience typical dynamical instability, but over time, the net growth of microtubule plus/minus ends is offset by continued shortening of minus/plus ends and resulting in the conservation of polymer mass. By assuming that there is an excess of GTP (guanosine triphosphate) available in the solution, and that the D-tubulin in the solution exchanges its unit of GDP (guanosine diphosphate) with a unit of GTP. By numerical analysis, the concentration of T-tubulin in the treadmilling steady state as a function of exchanges rate was investigated in the presence of free minus ends of microtubule (treadmilling steady state) and in the absence of free minus ends.

To conclude, by studying a biological system mathematically, we attempted to contribute to the understanding of the dynamics of microtubules. Mathematical models presented in this work are testable by experimental evidence. This may open a new window of predicting the polymer mass of microtubules using a given amount of anti-mitotic agent.

Bibliography

[1] Kirschner M., Michison T., Nature 312, 237 (1984).

[2] Pirolet F., Job D., Margolis R., and J. Garel, EMBO J. 6, 3247 (1987).

[3] Carlier M. F. et al., Proc Natl Acad Sci USA 84, 5257 (1987).

[4] Mandelkow E. M. et al., EMBO J. 7, 357 (1998).

[5] Lange G. et al., Eur. J. Biochem. 178, 61 (1988).

[6] Melki R., Carlier M. F., and Pantaloni D., EMBO J. 7, 2653 (1988).

[7] Mandelkow E. et al., Science 246, 1291 (1989).

[8] Wade R., Pirollet F., Margolis R., Garel J., and Job D., Biol. Cell 65, 37 (1989).

[9] Mandelkow E. M., Mandelkow E., Cell Motil. Cytoskeleton 22, 235 (1992).

[10] Carlier M. F. , Meiki R., Pantalini D. , Hill T. H., Chen Y., Proc. Natl. Acad. Sci. USA. 84, 5257 (1987).

[11] Dogterom M., Leibler S. Phys. Rev. Lett. 70 1347 (1997).

[12] Marx A., Mandelkow E. Eur Biophys J. 22 405 (1994).

[13] Houchmandzadeh B., Vallade M. Phys. Rev. E 53 6320 (1996).

[14] Jobs E., Wolf D. E.,Flyvbjerg H., Phys. Rev. Lett. 79, 519 (1997).

[15] Sept D., Limbach H. J., Bolterauer H., Tuszynski J. A., J. theor. Biol. 197, 77 (1997).

[16] Bolterauer H. et al., Journal of Biological Physics 25 (1999).

[17] Hill T. L., Proc. Natl. Acad. Sci. 81, 6728 (1984).

[18] Chen Y., Hill T. L., Proc. Natl. Acad. Sci. 82, 1131 (1985).

[19] Fygenson D. K., Braun E., Libchaber A., Phys. Rev. E 50, 2, (1994).

[20] Dogterom M., Yurke B. Phys. Rev. Lett. 81, 485, (1998).

[21] Flyvbjerg H., Holy T. E., Leibler S., Phys. Rev. E 54, 5538 (1996).

[22] Sept D., Phys. Rev. E 60, 1, (1999).

[23] Freed K. F., Phys. Rev. E 66, 061916, (2002).

[24] Dustin P. Structure and Chemistry of Microtubules in Microtubules, Springer-Verlag New York (1984).

[25] Jordan M. A., Wilson L., Nature Review Cancer 4, 253 (2004).

[26] Amos L. A., Trends Cell Biol. 5, 48, (1995).

[27] Horio T., Hotani H. Nature 321, 605 (1986).

[28] Walker R. A. et al. The J. Cell. Biol. 107, 1437 (1988).

[29] Desai A., Mitchison T. J., Annu. Rev. Cell. Dev. Biol. 13, 83, (1997).

[30] Correia J.J., Pharmacal. Therap. 52, 127 (1997).

[31] Nelson D. Mechanics of the Cell, Cambridge University Press, (2000).

[32] Timasheff S. N., Grisham L. M. Ann. Rev. Biochem. 49, 565, (1980).

[33] Correia J. J., Williams, R. C., Jr. Ann. Rev. Biophys. Bioeng. 12, 211, (1983).

[34] Engelborghs Y, in Microtubule Proteins, Avila, J.,Ed., CRC Press, Inc., Boca Raton, 1990, pp.I-35.

[35] Erickson H. P., O'Brien E. T., Ann Rev Biophys Biomol Struc 21, 145 (1992).

[36] Purich D. L., Kristofferson D. Adv. Protein Chem. 36, 133 (1984).

[37] Correia J. J., Lobert S. Current Pharmaceutical Design, 7, 1213 (2001).

[38] Lobert, S., Correia J. J., Meth Enzymology, Energetics of Macomoulecular, Part C, 323, 77 (2000).

[39] Lobert S., Fahy J., Hill B.T., Duflos A., Etievant C. Correia J.J. 39, 12053 (2000).

[40] Engelborghs Y. Eur. Biophys. J., 51, 377 (1998).

[41] Dowing K. H., Nogales E., Eur. Biophys. J. 27, 431-436 (1998).

[42] Gajate C., Barasoain I., Andreu J. M., Mollinedo F. 60, 2651 (2000).

[43] Panda D., Daijo J. E., Jordan M. A., Wilson L. 34, 9921 (1995).

[44] Mishra P. et al. 2003 arXiv:cond-mat/0310546.

[45] Caudron N., Valiron O., Usson Y., Valiron P., Job D., Biochem. J., 297, 211 (2000).

[46] Vandecandelaere A. et al. Biochem. J. 33, 2792 (1994).

[47] Vandecandelaere A., Martin S. R., Engelborghs Y. , Biochem. J. 323, 189 (1997).

[48] Govindan B. S., Spillman W. B. Phys. Rev. 70 32901 (2004).

[49] Waterman-Storer C. M., Sanger J. W., Sanger J. M., Cell Motil Cytoskel, 26, 19 (1993).

[50] Rodionov V. I, Borisy G. G. Nature 386: 215 (1997)

[51] Keating T. J., Peloquin J. G., Rodionov V. I., Borisy G. G., Proc Nat Acad Sci USA 90 (1997).

[52] Clare M. Waterman-Storer and E. D. Salmon Current Biology 7: R 369 (1997).

[53] Hammele M., Zimmermann W., Phys. Rev. E 67 21903 (2003).